Clouds and the Earth's Radiant Energy System (CERES)

Validation Document

Surface and Atmospheric Radiation Budget (SARB)
Validation Plan for CERES Subsystem 5.0
(Compute Surface and Atmospheric Fluxes)

T. P. Charlock
NASA Langley Research Center
Hampton, Virginia 23681-0001

F. G. Rose, D. A. Rutan, C. K. Rutledge, and K. Larman
Analytical Services and Materials, Inc.
Hampton, Virginia

Yongxiang Hu
NASA Langley Research Center
Hampton, Virginia 23681-0001

Seiji Kato
Hampton University
Hampton, Virginia

Martial Haeffelin
Virginia Polytechnique Institute
Hampton, Virginia

Release 4.0
October 2000

Validation of CERES Surface and Atmospheric Radiation Budget SARB (Subsystem 5.0)

5.1 Introduction

5.1.1 Measurement and Science Objectives

This document presents validation plans for the Clouds and the Earth's Radiant Energy System (CERES) retrieval of the vertical atmospheric profile of shortwave (SW, solar wavelengths) and longwave (LW, thermal infrared wavelengths) radiative fluxes: the Surface and Atmospheric Radiation Budget (SARB). The vertical profile of fluxes is calculated with satellite imager-retrieved clouds and meteorological data as inputs; the initial unconstrained radiative transfer calculations generally do not match the observed CERES TOA fluxes. The input parameters are then partially constrained to match the modeled TOA fluxes with the observed CERES broadband TOA fluxes. The unconstrained fluxes, constrained fluxes, and adjustments to inputs are archived for diagnostic studies of the radiative transfer techniques, the CERES cloud retrievals, and other parameters.

The CERES effort to retrieve surface radiative fluxes includes algorithms for (a) the full vertical profile of fluxes in the atmosphere and at the surface, determined from radiative transfer calculations that match the simultaneously observed CERES Top-Of-the-Atmosphere (TOA) fluxes, dubbed “SARB” (Subsystem 5.0); (b) an independent, parameterized set of radiative fluxes at just the surface, that are also simultaneous with the CERES TOA fluxes, dubbed “Surface-only” or “Surface Radiation Budget SRB” (Subsystem 4.6); and (c) both “SARB” and “Surface-only” for synoptic times, i.e., 3-hourly UTC (Subsystem 7.0). This document addresses primarily “SARB”, which uses radiative transfer algorithms similar to those in GCMs.

There are formidable challenges to developing accurate SARB records in CERES or in the Earth Observing System (EOS) generally. While certain components of the SARB can now be determined to useful accuracy with existing data, other components will be advanced, but not be resolved sufficiently, by TRMM, Terra, and Aqua. For example, to validate retrievals of the vertical profile of radiative fluxes, we will require the deployment of active remote sensing systems on satellites, such as the Cloud Profiling Radars (CPR) and cloud lidars like PICASSO-CENA and GLAS, to achieve time mean accuracies of better than 10 Wm-2/km (divergence for layers of 1 km thickness in the troposphere).

The detection of long-term trends within the atmosphere is an even more ambitious goal. Here we are sorely limited by the quality of available in situ radiometers. The best broadband instruments for radiation cannot approach the accuracy (per cent error) that can be

obtained with a well calibrated mercury thermometer for temperature. The stable CERES broadband radiometers are still capable of detecting interannal variations at TOA to a fidelity of about 0.25%; this is much better than the absolute accuracy of the measurement (~1%) at any given time. But detecting interannual variations to 0.25% at the surface or within the atmosphere (i.e., parsing a 0.25% signal at TOA between the surface and the atmosphere, as in direct aerosol forcing to scattering versus absorption) is much more difficult. While CERES will estimate this, the community will not accept the results with confidence until a new generation of more stable in situ radiometers have been developed and deployed in surface networks, permitting us to validate the results.

Despite such limitations, CERES will expand the space and time domain wherein the SARB can be determined to useful accuracy. The TOA fluxes computed in this component of CERES will be used for diagnostic applications; the difference, on a global scale, between modeled and observed fluxes will be a mark of our understanding of some of the most critical physical processes in climate change. The CERES program will not only provide accurate TOA broadband fluxes and simultaneous cloud property retrievals, but will also be well suited to consistently estimate the effects of clouds, gases, aerosols, and the surface on the various components of the SARB. The CERES SARB product will be a tool for resolving the uncertainties in climate analysis and climate prediction that are associated with (1) feedbacks due to clouds, water vapor, snow, and ice and (2) anthropogenic forcings due to aerosols, surface albedo, and ozone; for testing the current generation of climate and NWP models; for studies of circulation and the hydrological cycle; and to point the way to the new measurement technologies that are needed.

The validation of EOS is an opportunity to expand the observing capabilities of spacecraft by integrating satellites with surface and airborne measurements in a cost effective manner. Modest enhancements to existing and planned surface networks will permit CERES to monitor elusive climate forcings due to anthropogenic aerosol and changes in land use. Plans for this post-launch application are sketched in the section on "Class 2 Regional Climate Trend" sites. Validation of this component of CERES began well before launch with the on-line CERES/ARM/GEWEX Experiment (CAGEX; Charlock and Alberta, 1996).

5.1.2 Missions

CERES (Wielicki and Barkstrom, 1991) is a follow-on to the measurement of broadband TOA fluxes in (Barkstrom et al., 1989; Harrison et al., 1990). CERES will also simultaneously retrieve cloud properties with satellite imager data (Wielicki et al., 1995): the VIRS imager (similar to AVHRR) on the TRMM for 1997 launch and the MODIS (which has more channels than AVHRR and higher spatial resolution) on Terra (formerly EOS-AM), which was launched in 1999, and on Aqua (previously named EOS-PM). The calculation of the SARB, consistent with the measured broadband TOA fluxes and cloud property retrievals, is a small component of CERES (Charlock et al., 1997; Subsystem 5.0 ATBD).

5.1.3 Science Data Products

The SARB component of CERES retrieves the vertical profiles of SW and LW fluxes from the surface to the TOA. Upwelling and downwelling fluxes at the surface, 500-hPa, 200-hPa, 70-hPa, and TOA will be archived. Earlier documentation on Subsystem 5.0 noted that fluxes would be retrieved at the “tropopause”. We have since selected two fixed, levels, 200-hPa and 70-hPa, to respectively represent the approximate pressure altitudes of the extratropical and tropical tropopause. As the experiment matures, fluxes will be validated at a larger number of vertical levels. The ratio of upwelling and downwelling broadband SW flux at the ground is the surface albedo. Unlike the surface spectral reflectance, the surface albedo is not a property of the surface only; surface albedo depends on the downwelling flux, whose spectral and directional characteristics are influenced by the atmosphere.

The SARB fluxes are produced by plane parallel radiative transfer calculations (Fu and Liou, 1993; Fu et al., 1997, 1998, 1999) using CERES cloud retrievals (based mostly on a narrowband imager, Minnis et al., 1997) and other EOS data. The SARB fluxes are constrained to match the CERES observed radiation at TOA; the constrainment determines a match to TOA observations within an anticipated uncertainty sigma. A constrainment algorithm is used to select which input parameters (i.e., cloud optical depth, surface skin temperature) are to be adjusted (Rose and Charlock, 1997; Charlock et al., 1997). The SARB results are sensitive to both the values of the input data used for constrainment and to the apriori uncertainty (sigma) for those parameters. The adjusted (constrained) values for other quantities, such as the humidity sounding and aerosol optical depth, are validated informally.

For clear sky footprints over the ocean, the constrainment adjusts the surface skin temperature, lower tropospheric humidity (LTH), upper tropospheric humidity (UTH), and aerosol optical thickness (AOT) using CERES TOA observations of LW broadband radiance, 8-12 micron window

radiance, and SW irradiance. For clear footprints over land, the surface albedo is also adjusted; and the sigma (a priori uncertainty) for skin temperature is increased, causing a larger adjustment in skin temperature than over the ocean. For cloudy or partly cloudy footprints, the parameters used to tune clear footprints are frozen; cloud optical depth, cloud fractional area, and cloud top height are adjusted instead.

To permit the user to infer cloud forcing and direct aerosol forcing, the archive includes surface and TOA fluxes that have been computed for respectively cloud-free and aerosol-free conditions. This component of CERES also produces and validates the surface photosynthetically active radiation (PAR; 0.4-0.7 micrometer). Surface UV (i.e., Lubin et al., 1998; Li et al., 2000) will be an experimental product.

Table 1 Place of Surface and Atmospheric Radiation Budget (SARB) in one portion of CERES processing

	CERES radiance SW,LW,window (Wm-2sr-1)	angular models ----------> used by ERBE	"ERBE-like" ES8 TOA flux (Wm-2)	*in archive*
in progress	VIRS or MODIS + ECMWF T(z)	---------->	Cloudiness (area, height, LWP, IWP)	
in progress	Cloudiness + CERES radiance	new angular ----------> models	More accurate TOA fluxes ~ 2000-1	
in progress	TOA fluxes + CERES clouds + T,H2O,O3(z)	rad. trans. ----------> + adjustment	"SARB" flux profiles ~ 2001-2	tuned clouds, aerosols, PW, skin T archived

5.2 Validation Criterion

5.2.1 Overall Approach

The irradiance profile in the SARB component of CERES is the output of a theoretical radiative transfer calculation. As such, there are two principal sources of error (Liou, 1992): the radiative transfer code and the inputs for that code. While we are able to validate a tiny fraction of this output directly with measurements of broadband fluxes, there are limitations to both the accuracy and spatial representativeness of such available in situ measurements. We therefore also emphasize validation of the radiative transfer model and the inputs for the code (see Table 2).

Table 2 Components of SARB validation

Radiative transfer code Insert diagnostics Test and improve Accessible to community at SARB group URL	Inputs for calculation Local scale tests Global scale tests On-line access to some inputs at CAVE URL
Space-time sampling TOA: global CERES match Surface: continuous In-atmosphere: balloon (ULBD)& aircarft	In-situ measurements Network collaboration Instrument assessment Low-level OV-10 plane Sea platform (COVE)

Early validation relied heavily on the use of data sets and programs which were not supported directly by EOS; for example, the measurements of surface fluxes and other parameters collected by ARM. We interact with other programs, such as GEWEX, by providing carefully honed and readily accessible CERES products to users who then effectively participate in CERES development, and eventually validation. This approach began well before the 1998 launch of TRMM with the CERES/ARM/GEWEX Experiment (CAGEX; Charlock and Alberta, 1996), a temporally intensive, limited area data set that is available online (http://snowdog.larc.nasa.gov:8081/cagex.html). CAGEX Versions 1 and 2 provide a record of fluxes which have been computed with a radiative transfer code; the atmospheric sounding, aerosol and satellite-retrieved cloud data on which the computations have been based; and validating surface-based measurements for radiative fluxes and cloud properties from ARM. Version 1 (2) of CAGEX covers April 5-30, 1994 (Sept. 25 - Nov. 1, 1995). NCEP and ECMWF have both found CAGEX to be useful for testing components of NWP models.

Based in part on the pre-launch CAGEX, CERES collaborated in improving successive versions of the Fu-Liou radiative transfer code (i.e., including the Chou and Suarez, 1999 treatment of the absorption of SW by CO2); initiated a shift to a new source of NWP data (ECMWF, Rabier et al., 1998) for providing needed atmospheric soundings; and prompted the community to seek improved measurements of a fundamental quantity, the surface broadband solar insolation (i.e., Haeffelin et al., 2000).

By agreement with Prof. Qiang Fu, CERES maintains a "point and click" version of the Fu-Liou code for on-line calculations at the SARB Working Group (WG) URL (srbsun.larc.nasa.gov/sarb/sarb.html). A useable version is available through e-mail concurrence of Prof. Fu and the SARB WG at Langley.

Most of the data for post-launch validation of fluxes has been obtained from measurements by ARM (DOE); the NOAA Climate Monitoring and Diagnostics Laboratory (CMDL, i.e., Dutton et al., 2000); the NOAA SURFRAD (Hicks et al., 1995, Augustine et al., 2000); the National Renewable Energy Laboratory (NREL, Myers et al., 1999); a University of Maryland site at Ilorin, Nigeria; a special, local program at the Chesapeake Lighthouse (CERES Ocean Valiation Experiment COVE); and other sites of WCRP Baseline Surface Radiation Network (BSRN; DeLuisi, 1991; Gilgen et al., 1995). EOS resources are needed to purchase supplementary instruments for some of these sites; others need support for the basic integretity of their measurements.

The accuracy and stability of the time series of broadband in situ measurements are of paramount importance. Raw accuracy of the surface measurement is needed, for example,to validate the radiative transfer code. Stability (precision) of measurement is needed to a higher degree, as there are other applications. If the in situ measurements were stable for a long period at a site, a purported secular trend in say, aerosol forcing, retrieved by SARB could be checked; one could then extend (or contest) the SARB record of aerosol forcing for a larger area about the site. To foster both this type of analysis and the improvement in supporting measurements, we have developed an on-line record of suitably formatted validation data at SURFRAD, CMDL, NREL, ARM, and other sites (CERES ARM Validation Experiment CAVE at the URL www-larc.nasa.gov/cave/). CAVE contains easy-to-use subsets of collocated CERES TOA for each surface validation site.

CAGEX Version 2 (Table 3) covered the first ARM Enhanced Shortwave Experiment (ARESE) field campaign. Our experience with validation using long-term networks, short-term field campaigns, and the even shorter domain aircraft measurements lead us to stress the application of long-term networks. Issues like cloud inhomogeneity (i.e., Fu et al, 2000) argue for the use of a substantial domain when validating a retrieval that is largely based on plane parallel radiative transfer. We leverage resources for

field campaigns with a goal to improving the interpretation of measurements taken by continuous networks; for example, our August 1998 helicopter survey of the surface albedo in the vicinity of the ARM SGP Central Facility (Major et al., 1999). Given the discrepancies of measurement and theory for existing surface data (see next section), we cannot presently advocate an extensive, independent campaign with powered aircraft to validate the retrievals of fluxes at different levels within the atmosphere. We will include aircraft measurements of broadband flux profiles in our own field campaigns when this can be done economically. Measurements of in-atmosphere fluxes by aircraft experiments such as CRYSTAL will be used as opportunities arise. The on-line "CAVE" (see next page Figure 1 and Table 3 below) is the main access point to these activities. The "CLAMS" (Table 3) field campaign will be described later.

Table 3 CERES Validation Activities

CAVE
CERES ARM Validation Experiment
40+ sites: SURFRAD, CMDL, ARM & BSRN
30-min surface fluxes & collocated CERES TOA when available
Continuous from Jan. 98
On-line access

CAGEX
CERES ARM GEWEX Experiment
Focus on ARM SGP Central Facility
Computed flux profiles, inputs & measurements for validation
April 1994 & Fall 1995
On-line access

COVE
CERES Ocean Validation Experiment (Chesapeake Lighthouse)
Long-term, continuous, collocated, calibrated radiation at sea
All-sky SW&LW, aerosols surface boundary cond.

CLAMS
Chesapeake Lighthouse & Aircraft Measurememnts for Satellites
Summer 2001 field campaign CERES, MISR MODIS, and GACP
Clear-sky SW & aerosols over ocean

Figure 1 (next page) **Overview of the on-line CAVE**

NASA Langley CERES ARM Validation Experiment
CAVE

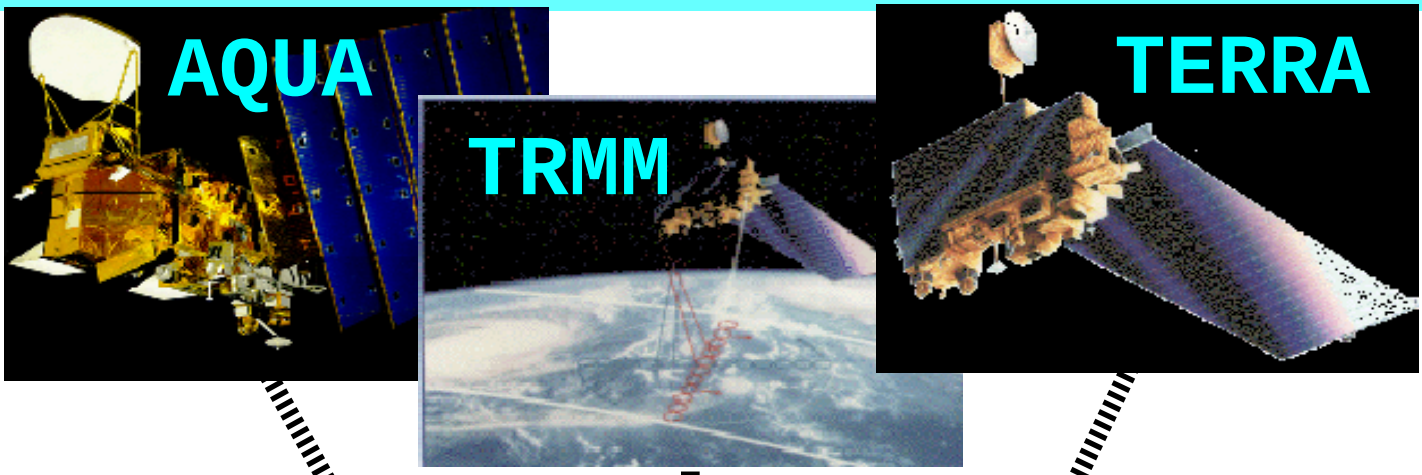

Top of Atmosphere Broadband Radiation

Calibrated

Collocated

Closure for Net Atmospheric Radiation

Continuous

Long Term

Surface Broadband Radiation

Global Sites

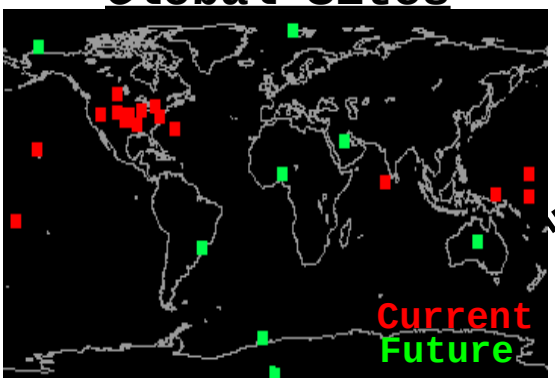

ARM Oklahoma Network

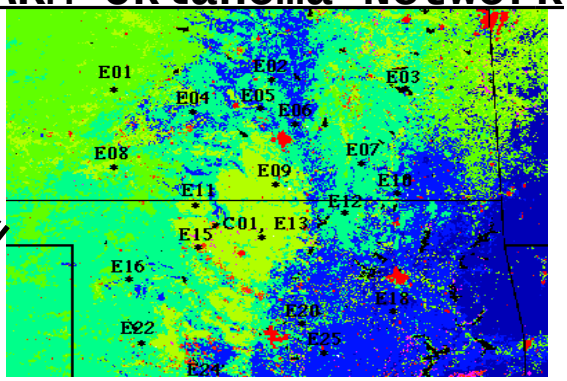

CAVE provides on-line surface and collocated CERES data at over 30 sites worldwide (ARM+SURFRAD+CMDL+BSRN)

http://www-cave.larc.nasa.gov/cave/

5.2.2 Accuracy of Current State of the Art

5.2.2.1 TOA Fluxes

Estimates for the error in the TOA budget with ERBE (Barkstrom, 1989) range from about 5-8 Wm^{-2} for the net (SW+LW) budget of the global annual mean to approximately 30-50 Wm^{-2} for the instantaneous footprint-scale SW flux, where the inversion process shows a strong dependence on the angular and directional model ADM (Suttles et al. 1988; 1989) and the scene identification (Wielicki and Green, 1989). Errors in the CERES initial round of processing (called "ERBE-like" and ES8 on the DAAC archive) are comparable. The CERES goal is to reduce such errors by at least a factor of two, with more advance processing of the same TOA measurements. The new TOA products, which are called SSF, are used in SARB. Figure 2 compares a preliminary set of observed SSF tropical ocean (TRMM) fluxes with Fu-Liou calculations. Computed fluxes are here untuned: the constrainment algorithm has not been applied to adjust the inputs in Figure 2 (see next page **Figure 2 Comparison of untuned Fu-Liou calculations with CERES TOA observations**).

For clear sky SW, the computed values for reflected flux are large by a mean 2 Wm-2; this is partly due to a coding error for the surface albedo over a relatively small number of points (upper right panel of Figure 2). While the computation for reflected SW under total-sky conditions (upper left panel of Figure 2) has a mean that is only 4 Wm-2 larger than observations, the standard deviation of the difference (observed minus computed) is larger at 37 Wm-2. This supports the error estimate of 30-50 Wm-2 for the instantaneous footprint-scale SW.

For total-sky OLR in Figure 2, the mean computed value exceeds the observations by only 2 Wm-2 (lower left). But for low values of total-sky OLR, computations exceed observations by quite a lot. The error for computed total-sky OLR exceeds 10 Wm-2 when the domain is confined to overcast ice clouds only (not shown). The LW computation uses a 2/4 stream (Fu et al., 1997) approximation, wherein an economical 2-stream phase function is then used for two quadrature directions up and two quadrature directions down (as in a 4-stream computation). We are now checking the current version of our fast code with a 16 stream discrete ordinate model (Stamnes et al., 1988); earlier versions were tested in Intercomparison of Radiation Codes in Climate Models (ICRCCM; Ellingson and Fouquart, 1990; Ellingson et al., 1991). Ice crystals are here assumed to have random geometric orientation, which would be valid for small particles. For larger particles, the assumption of random orientation could generate a large error, but more for reflected SW than for OLR. Interestingly, we do not

DAYTIME OCEAN Full SKY SW REFLECTED

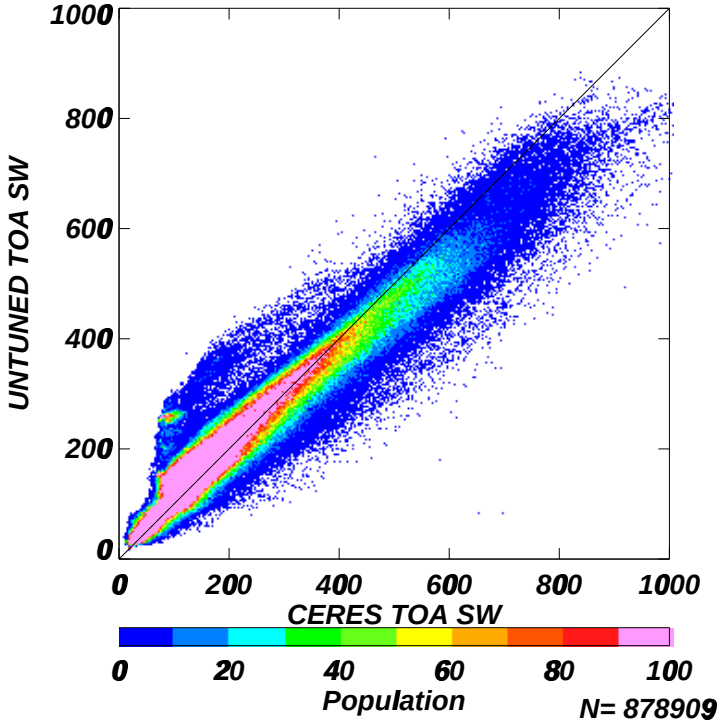

N= 878909
Mean (Std.Dev)
CERES TOA SW : 178.11 (151.83)
UNTUNED TOA SW : 182.12 (138.03)
X - Y : -4.02 (37.02)

DAYTIME OCEAN Clear sky SW REFLECTED

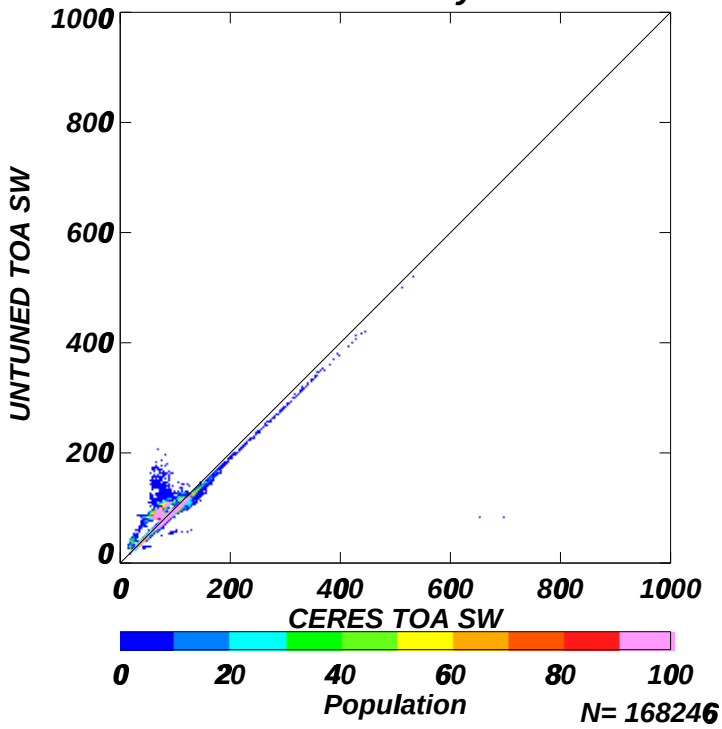

N= 168246
Mean (Std.Dev)
CERES TOA SW : 75.61 (19.89)
UNTUNED TOA SW : 77.73 (19.38)
X - Y : -2.12 (7.74)

DAYTIME OCEAN FULL SKY OLR

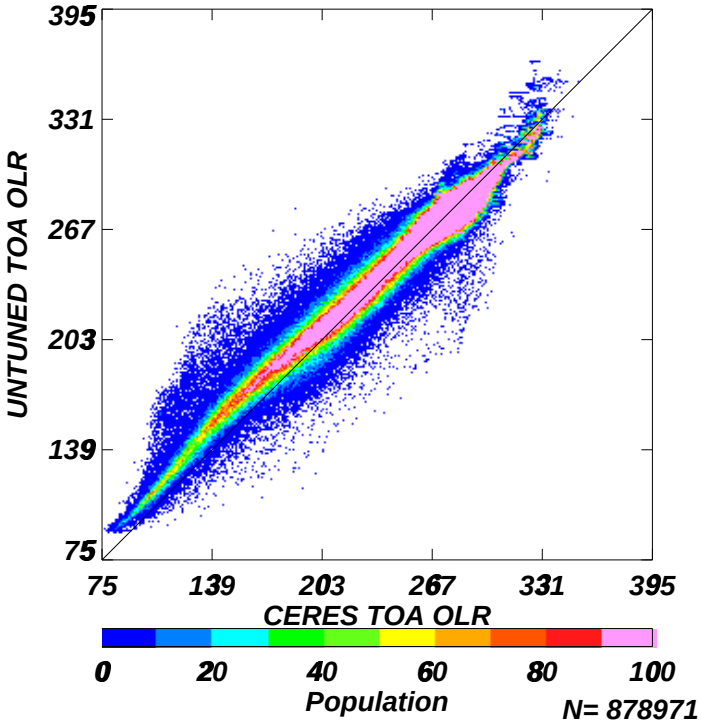

N= 878971
Mean (Std.Dev)
CERES TOA OLR : 256.44 (45.13)
UNTUNED TOA OLR : 258.72 (40.57)
X - Y : -2.34 (9.14)

OCEAN CLEAR SKY OLR

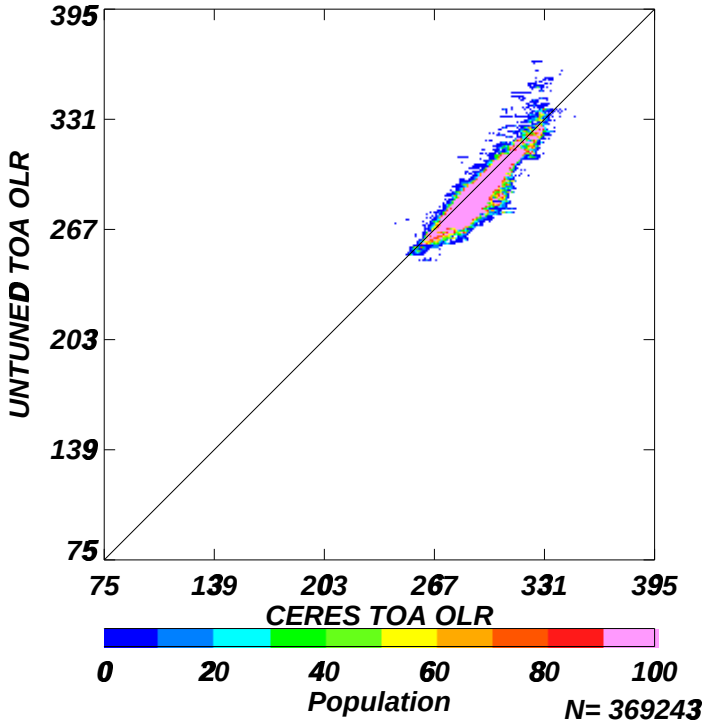

N= 369243
Mean (Std.Dev)
CERES TOA OLR : 291.50 (12.06)
UNTUNED TOA OLR : 288.69 (13.15)
X - Y : 2.80 (5.17)

find large discrepancies between observation and simulation for SW when overcast ice clouds are isolated (not shown).

The comparison of computed and observed OLR for clear sky over the ocean in Fig. 2 is quite favorable. The few points with great error are obviously due to cloud contamination, where the computed values are expected to exceed observations. The standard deviation for computations versus observations is only 5 Wm-2. A study of the earlier ERBE clear sky OLR (Collins and Inamdar, 1995) anticipated deviations of up to 20 Wm-2 due to the ADM in particular conditions of humidity. Here we have used ECMWF temperature and humidity profiles (Rabier et al. 1998). The direct assimilation of TOVS water vapor radiances by ECMWF appears to have delivered a humidity profile that is quite consistent with the Fu-Liou code and new CERES observations. The good match of computed and observed OLR for clear conditions is partial validation of the retrieved in-atmosphere cooling rates (i.e., LW divergence between 200 hPa and 500 hPa, two levels for archival of flux profiles). The constrainment algorithm (not applied for Figure 2) plays off the difference between simulated and observed broadband LW and 8-12 micrometer window (WN) radiances by adjusting lower tropospheric humidity (LTH) and upper tropospheric humidity (UTH), improving the match of computations and measurements.

5.2.2.2 Surface shortwave fluxes

On a monthly average for a 2.5 deg by 2.5 deg grid, it is often assumed that the 1980s ERBE fluxes are correct to within approximately 10 Wm^{-2} (Harrison et al., 1991). The error in the surface flux inferred ERBE or other satellite data is larger. Using the algorithms due to Darnell et al. (1992) and Pinker and Laszlo (1992), the analyses in Whitlock et al. (1995) suggest that the rms error in the surface SW flux is roughly 20 Wm^{-2} for the monthly average for a 280 by 280 km equal area ISCCP (Rossow et al., 1991) grid; the bias is 10-15 Wm^{-2}. Li et al. (1995a) use ERBE data and optimistically report a smaller bias for the global mean surface SW flux. Satellite-based retrievals of the surface radiation budget have some skill in monitoring the interannual variability (IAV) – provided that the signal is strong enough. Alberta et al. (1994) used GEWEX SRB Project retrievals based on the operational satellite record from ISCCP (Rossow et al., 1991) and demonstrated consistency with surface measurements for a ~30 Wm-2 excursion in the surface insolation over West Europe from the spring means in 1985-86 versus 1987-88.

5.2.2.3 Shortwave in cloudy skies

Such estimates for the error in satellite-retrieved surface SW flux have met a significant challenge, however. Cess et al. (1995), Ramanthan et al. (1995), and Pilewskie

et al. (1995) advocate a strong role for the absorption of SW radiation by cloudy skies; the cloud forcing of the absorption of SW radiation by the atmosphere is inferred to have a global mean value of 25-40 Wm^{-2}. In turn, these results have been contested, by the aircraft observations of Hayasaka et al. (1995), and questioned by Chou et al. (1995) using theory. Aircraft data in the specially commissioned ARESE (1995) campaign were then used by Zender et al. (1997) and Valero et al. (1997), who both deduced extraordinary absorption by cloudy skies over Oklahoma. The issue for CERES is simply that the retrieved atmospheric absorption is based on theory (the Fu-Liou code), and theory does not produce extraordinary atmospheric absorption in cloudy skies. Li et al. (1995) sugggested a role for aerosols in such “anomalous” cloud absorption.

CAGEX found no evidence for extraordinary cloud forcing to SW absorption in the time mean of both Versions 1 (covering April 1994) and 2 (Fall 1995); this used GOES narrowband data (Minnis et al., 1995) as a surrogate for broadband at TOA, broadband ARM SIROS observations at the surface, and compared the resulting atmospheric absorption with theory. But for the very few days targeted by ARESE (i.e., Zender et al., 1997 and Valero et al., 1997), CAGEX Version 2 indeed found that the observed atmospheric absorption for cloudy skies exceeded computations by ~80 Wm-2 (Charlock et al., 1998); theory and observation could be reconciled only by assuming the presence of strongly absorbing aerosol particles within the clouds; the measurements of aerosols that would be needed to resolve this are not available. Valero et al. (2000) carefully re-examined the 1995 ARESE flight data and stated that, they are consistent with the original finding of extraordinary absorption by cloudy skies.

As in the pre-launch CAGEX, an examination of CERES ES8 (“ERBE-like”) over SGP also finds no extraordinary cloudy-sky absorption by the atmosphere (Charlock et al., 1999). Results for a few thousand collocations of CERES TOA (instantaneous snapshots) and ARM SIRS net surface fluxes are summarized in Table 4. Cloud screening is done with two independent techniques; the satellite-based Maximum Likelihood Estimator (MLE) of Wielicki and Green (1989); and the Long and Ackerman (2000) objective analysis of time series of surface pyranometer data. The coarse MLE, which does not use high resolution VIRS cloud imager data, appears to produce a “clear sky” which is roughly equivalent to the cloud fractional coverage of 0.15 according to the surface time-series analysis. The cloud forcing (total sky minus clear sky) is 8 Wm-2 (mean cosSZA 0.63) with the MLE and 23 Wm-2 (mean cosSZA 0.61-0.63) for the Long and Ackerman (2000) screening. These scale, respectively, to cloud forcings of only 3 Wm-2 and 9 Wm-2 for the global annual mean cosSZA of 0.25; and are much smaller than the 25-40 Wm-2 forcing advocated for the

global annual mean as interpreted from the 1995 Science papers. A recent aircraft experiment (Asano et al., 2000) also finds no extraordinary solar absorption by clouds.

Table 4

SW Atmospheric Absorption CERES and ARM SGP (Jan.-Aug. 1998)

MLE = CERES "ERBE-like" cloud screening

Long = Clouds screened with surface flux time series

= number of collocations for satellite at 21 surface sites

parameter	MLE	#	Long 0.00	#	Long 0.05	#	Long 0.15	#
Atmosphere abs.	Wm-2		Wm-2		Wm-2		Wm-2	
total sky	227.3	6317	227.3	6317	227.3	6317	227.3	6317
clear	218.8	1888	148.1	349	198.4	1427	204.0	1928
cloud forcing	8.5		79.2		28.8		23.3	
CosSZA(total sky)	0.63		0.63		0.63		0.63	
CosSZA(clear sky)	0.63		0.43		0.60		0.61	
cloud forcing scale								
to CosSZA=0.25	**3.36**						**9.41**	

5.2.2.4 Shortwave in clear skies

A study of GCM codes (Wild et al., 1995) and the first CAGEX results (Charlock and Alberta, 1996) both indicated that calculated SW insolation for clear sky conditions significantly exceeds measured values. Kato et al. (1997) suggested the presense of an unidentified absorber to account for the discrepancy (~20-30 Wm-2), which is found mostly in the diffuse (rather than the direct) component of the beam. Halthore et al. (1998) considered a possible role for aerosols in the discrepancy. Reports of the discrepancy are not univeral (Zender et al., 1997). Kato et al. (1999a) found no discrepancy for a molecular atmosphere at Mauna Loa with few aerosols, but reported another significant discrepancy for cases in Oklahoma with aerosols (Kato et al., 1999b).

Alberta and Charlock (1999), Bush et al. (2000), Haeffelin et al. (2000), and Dutton et al. (2000) found that adjustments for "thermal IR offset" were needed to the record of the shaded Eppley PSP, which measures the diffuse insolation. Wild et al. (1998, 1999) do not find significant disagreement between theory and measurements by the shaded pyranometer of Kipp and Zonen, which has a

smaller thermal offset than the Eppley PSP. In most cases, the thermal offset causes the PSP instrument to produce a flux that is too low; correcting for thermal offset improves the match with calculations. This instrument characteristic accounted for some of the discrepancies reported by CAGEX Version 1 and Kato et al. (1997). The current Version 2 of CAGEX and most of the sites at our CAVE data base have been corrected at Langley (Alberta and Charlock, 1999) using the methods of Dutton et al. (2000); the interested reader is directed to the CAGEX URL (www-cagex.larc.nasa.gov/cagex/) which has an immediate link to "treatement of diffuse flux". The NOAA CMDL validation sites at Bermuda, Kwajalein, Mauna Loa and Boulder now measure the diffuse component of insolation with the Eppley Black and White (B&W) sensor, for which the thermal offset is minimal. NOAA SURFRAD sites are expected to deploy Eppley B&W sensors during the coming year.

A comparison of measured and computed insolation illustrates how a satellite-based retrieval is expected to perform under ideal conditions: when radiative transfer inputs like aerosol optical thickness (AOT) and precipitable water (PW) are determined from reliable field measurements. In Table 5 for January 1999 to May 2000, observations (OBS) of surface radiation are taken from 30-minute means (adjusted and stored at the on-line CAVE) at the ARM SGP "E13" SIRS facility collocated with the Central Facility (CF) "C01". For the radiative transfer computation, CF radiosonde data is used for the water vapor profile after an adjustment to total PW using the SGP Microwave Radiometer (MWR); alternately MFRSR (Harrison et al., 1994) and Cimel (Holben et al., 1998) surface photometers for spectral AOT; cloud screening from time series analysis of surface radiometer data (Long and Ackerman, 2000); the Stratospheric Ozone Monitoring Group Ozone Blended Analysis (SMOBA, Yang et al., 2000) from SBUV/2. Aerosol optical properties are assumed to be continental (d'Almeida et al, 1991) with 10% soot (Hess et al., 1998); this yields, for single scattering albedo at 565 nm, values that compare favorably with our preliminary analysis of Cessna flight profiles (year 2000 at SGP CF) mentored by John Ogren of CMDL. Spectral AOT in the photometer bands are taken from observations and spline fitted through the remainder of the spectrum. The highlighted box in Table 5 shows the results using the Cimel photometer for the full domain of 915 half-hourly intervals during 1999-2000.

Table 5 Clear Insolation Bias at ARM SGP CF (1999-2000)

Fu-Liou code using MWR PW AOT(MFRSR) and AOT(Cimel)

(Computed – Measured) in Wm-2

		full domain	|NIP1-NIP2| < 5 Wm-2	domain of Cimel V2.0
MFRSR	normal	10	6	16
	diffuse	3	4	1
	total	8	8	9
Cimel	normal	-2	-10	20
	diffuse	8	10	-1
	total	6	5	10
		Jan99 to May00 d'Almeida + 10% soot	two NIPs agree to 5 Wm-2	Jan99 to Mar99 calibrated Cimel

normal incidence pyrheliometer (NIP)
diffuse (shaded PSP corrected by Alberta-Dutton)
total = (NIP)*cos(SZA) + diffuse

The mean difference of only 6 Wm-2 (difference of computed and measured total insolation to a horizontal surface) belies aspects of the comparison that are revealed by examining the complete time series in Figure 3 (see next page). The observed total insolation is based on the recommended summation of two instruments. For the direct normal beam, the differences of computations and measurements are positive early in the record and negative later; for the diffuse insolation, we note the opposite; hence the agreement of computation and measurement for the mean is partly due to fortuitous compensation. At least one of the measurements must be drifting. If we based the analysis on a short field campaign of a few weeks, such a problem could be overlooked completely.

Figure 3 (see next page) **Difference as (Model minus Observations) for components of clear-sky SW at surface. ARM SGP CF 1999-2000.**

ARM_SGP_E13 : CIMEL(7)AOTs : Jan1999-May2000 Cave Flux Data
Sonde T(z),Q(z): MWRPW : SMOBA O3(z) : CLEAR C.Long<0.01

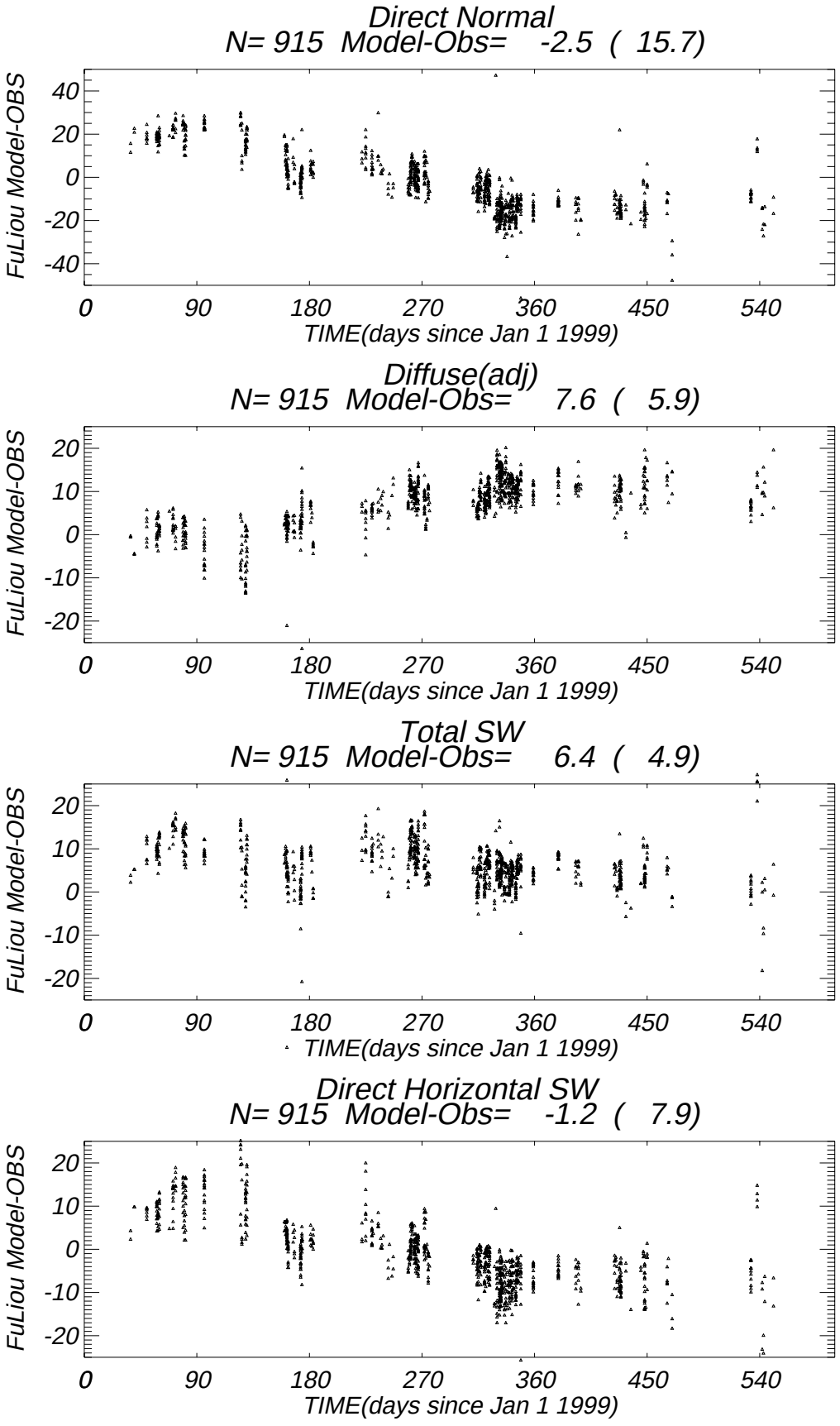

Table 5 also shows the results of additional tests. If the record of AOT from the MFRSR (Multifilter Shadowband Radiometer, Harrison et al., 1994) replaces the AERONET Cimel for the calculations with the Fu-Liou code, the computed direct normal beam is 10 Wm-2 higher than the observations, versus 2 Wm-2 lower than the observations with Cimel. Schmid et al. (1999) have noted limitations (~0.01-0.02) in the consistency of measurements for spectral AOT by photometers. There is presently no international protocol for the calibration of spectral photometers used to measure AOT.

The measurement of the direct normal by the NIP is probably the most highly regarded in this constellation of radiometric observations. The NIP can be can be calibrated with an Active Cavity Radiometer (ACR) and compared with the World Standard Group (WSG). The ACR is essentially a pyrheliometer without a protective window. Another NIP at site "C01" was effectively collocated with "E13" used in Figure 3. The middle column of Table 5 compares computed and measured fluxes for the period (567 half-hourly intervals) wherein both NIPs agreed to within 5 Wm-2; perhaps regular cleaning of the windows of both NIPs was then thorough. In this restricted domain, the discrepancy (calculations – observations) for the direct normal with the MFRSR is 6 Wm-2 versus –10 Wm-2 with the Cimel; a whopping algebraic distance of 16 Wm-2, simply by changing photometers. If we restrict the comparison to the shorter domain for which there is calibrated Cimel data (right column), the difference of calculation and measurement is not improved for the direct normal beam or the total horizontal beam, with either photometer.

Given these limitations for clear-sky insolation and the overall controversy for cloudy conditions (see earlier review by Stephens and Tsay, 1990), it is premature to confidently state the errors in the SW flux vertical profile at various levels within the atmosphere. But the difference of theory versus measurement can still provide a rough bound for the errors in quantitites like forcing. Aerosol forcing, for example, is the difference of theoretical fluxes computed with and without aerosols. How accurate are diagnosed aerosol forcings? Figure 4 (see next page) gives the aerosol forcing, scatter plotted versus AOT, for the domain of Figure 3 (the shaded area of Table 5). For each component of the flux, the estimated mean error (difference of model and observation) is less than the mean aerosol forcing for all but small AOTs.

Figure 4 (see next page) **Scatterplot of Model minus Observations (black) and Aerosol Forcing (red) versus Aerosol Optical Thickness AOT. Clear skies ARM SGP CF 1999-2000.**

ARM_SGP_E13 : CIMEL(7) AOTs: Jan1999-May2000 Cave Flux Data
Sonde T(z),Q(z): MWRPW : SMOBA O3(z) : CLEAR C.Long<0.01
N= 914

Direct Normal [Wm-2]
Model-Obs= -2.7 (13.9) Aerosol Forcing= -108.6 (43.3)

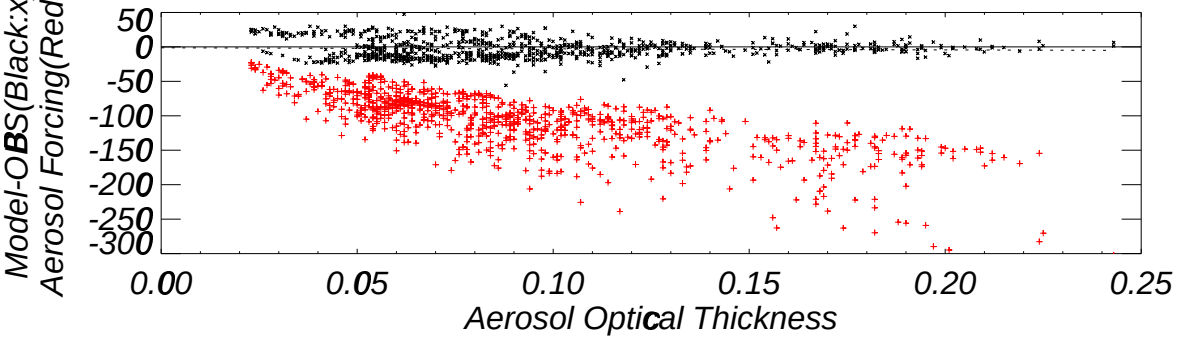

Diffuse(adj) [Wm-2]
Model-Obs= 7.6 (5.8) Aerosol Forcing= 37.3 (18.1)

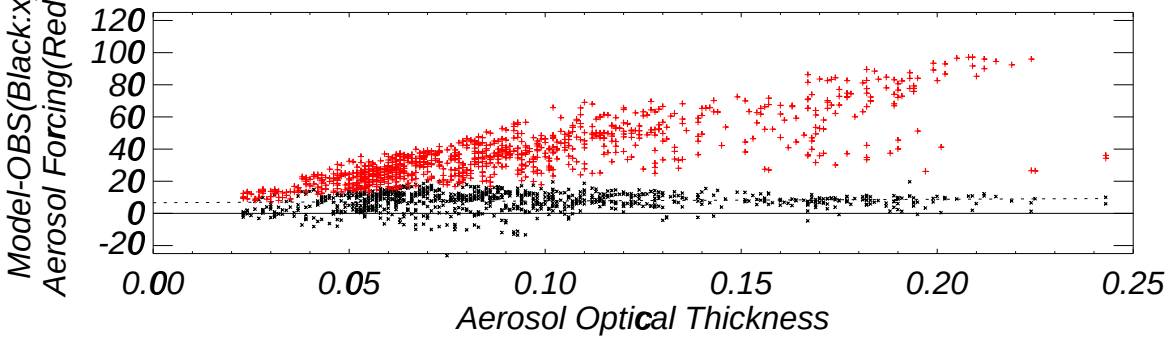

Total SW [Wm-2]
Model-Obs= 6.4 (4.9) Aerosol Forcing= -19.0 (7.6)

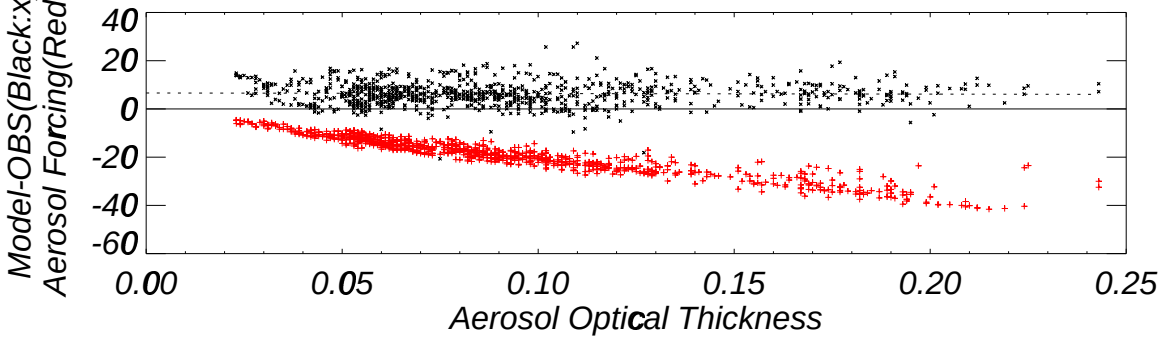

Direct Horizontal SW [Wm-2]
Model-Obs= -1.2 (7.7) Aerosol Forcing= -56.3 (25.3)

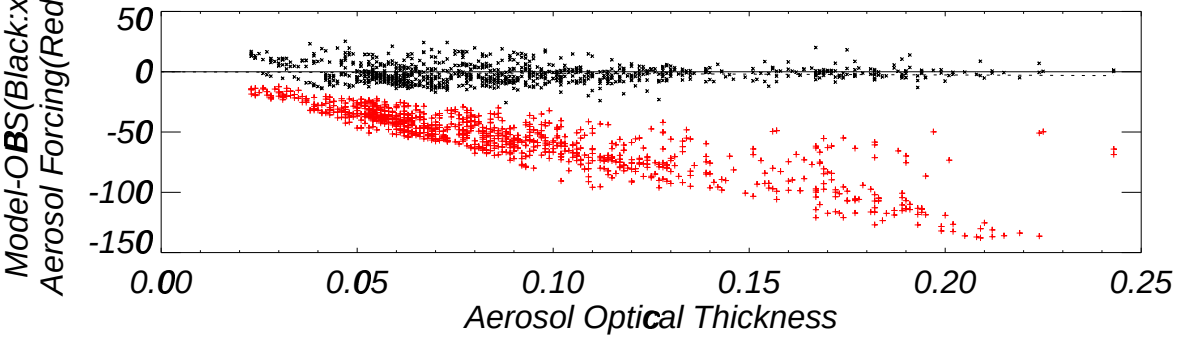

5.2.2.5 Longwave fluxes

Gupta (1989) estimated the errors in the LW surface flux associated with errors in atmospheric parameters used to calculate the flux. Surface and atmospheric temperatures were assumed to have random errors of about 2.5 K, producing errors of 7-13 Wm-2 in the downward and net LW flux at the surface for a range of atmospheric soundings. The errors in preciptable water (PW) were taken as 30%; if we assume a PW error of 15%, the corresponding error in the downward and net LW surface flux would range from 2-9 Wm-2. An error of 50 hPa in the cloud base height would typically produce an error of 1-3 Wm-2 the surface LW flux; an error of 10% in cloud cover would typically produces flux errors of 2-10 Wm-2; both of these cloud-induced errors are much larger for low clouds in a cold atmosphere.

Within the atmosphere, the divergence of LW flux is more physically significant than the net flux itself at an individual level. The divergence is usually expressed as a cooling rate. Uncertainty in the thickness and overlapping of cloudiness leads to an enormous uncertainty in the cloud forcing to the LW cooling rate of the atmosphere. With the atmosphere divided in even fairly thick vertical slabs of roughly 100 hPa, the error introduced by cloud overlap can exceed 0.25 K/day for a monthly average; this is 25% of the range of atmospheric LW cloud forcing (Charlock et al., 1994b). Systematic attempts to retrieve the vertical profile of fluxes began with operational satellite data (Stuhlmann et al., 1992; Ellingson et al., 1994).

Because of the great impact of rapidly varying cloud boundaries on both LW and SW divergence, an instantaneous estimate of divergence for a thin layer based on satellite data can have limited meaning; an extensive aircraaft campaign would be needed to validate a single retrieval. More credence can be obtained by integrating over time for thick layers. We can be more confident above the cloud tops, too. CERES should be able to retrieve LW and SW fluxes at the tropopause (which is above cloud top) with confidence at all time scales, thereby providing a reliable net radiation budget for the stratosphere. If coupled with a thorough validation program over sites having detailed measurements of radiation and aerosol properties, the CERES retrieval of divergence could also be a confident result in the troposphere for clear skies.

5.2.2 Sampling Requirements

Sampling for validation involves coverage of not only a single component of the radiation budget in space and time, but also collocated measurements of different components and some of the physical parameters that force those components. We focus on sites that measure several radiation parameters; and ideally redundantly (i.e., Table 5 uses both radiosonde and MWR data for humidity, MFRSR and Cimel for AOT, and collocated broadband pyrheliometers). Long-term measurements have the best prospect for reducing the error in sampling, and the use of multiple parameters (i.e., SW downwelling, SW net, SW direct, UV-B, PAR, aerosol photometer, cloud lidar, etc.) permits us to determine the physics of the process and tighten the drum on constrainment.

Figure 5 Contrasting inhomogeneity for two nearby land sites (L1 and L2) and two nearby sea sites (S1 and S2)

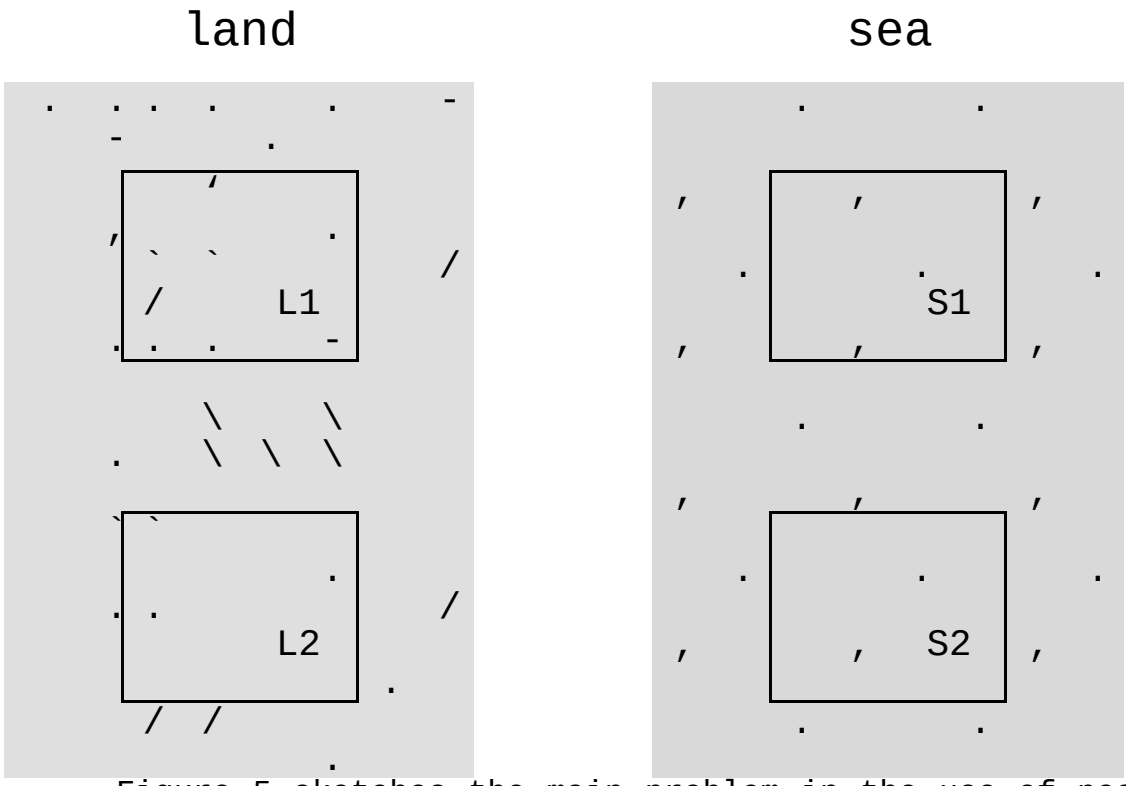

Figure 5 sketches the main problem in the use of near-surface based sensing for the validation of retrieved UPWELLING fluxes with satellite data. The spotty matrix of punctuation marks in the left column represents different types of soil, vegetation, and terrain that are directly beneath two land-based towers that measure upwelling flux. Over almost all vegetated surfaces, the shortwave radiation over one tower is different than that over another; if the upwelling fluxes are the same today, they will surely be different in a few months, after the canopy ages. Can one

ever be confident that the upwelling surface radiation at a single location will ever represent the mean surface radiation over a larger dimension of an entire satellite footprint? For downwelling fluxes, integration over time solves most of the problem over many locations (i.e., Barnett et al., 1998). But validation of satellite-based retrievals (area mean) of upwelling or net flux with surface-based instruments is problematic.

The sampling over the ocean (right column of Figure 5) is different. Ocean waves ensure that over two sites, some aspect of the upwelling surface radiation (direction or wavelength) will differ for any instantaneous snapshot. But if the two ocean sites are nearby, the time mean upwelling over one will represent the other very well; both will represent the time mean upwelling flux over a larger area, such as a MODIS footprint (~1km). Because of this unique characteristic of radiation over the sea, we have established the CERES Ocean Validation Experiment (COVE) at the Chesapeake Lighthouse (Figure 6 see next page).

NASA Langley Research Center (LaRC) has an agreement with the United States Coast Guard (USCG) for continuous access to the Chesapeake "Lighthouse" ocean platform during the next 15 years. The stationary platform is located 20 km off the coast, due east of coast Virginia Beach, and approximately 450 km west of the continental shelf transition. The water depth at COVE is 11 m. COVE instruments on the platform are usually deployed 15-25 m above the sea surface, well above the most intense ocean spray. Several measurement programs use the facility. The National Data Buoy Center (NDBC) has made standard meteorological and ocean surface wave energy measurements for over fifteen years at the site.

CERES has installed a Baseline Surface Radiation Network (BSRN) measurement station at COVE for broadband fluxes, supplemented with an MFRSR photometer for spectral AOT; the submission of data to the BSRN archive began in August 1999. The broadband downwelling measurements include direct SW, shaded diffuse SW, unshaded SW and shaded LW; upwelling broadand SW and LW. Upwelling broadband SW and LW fluxes are measured on the westernmost side of the COVE platform; there is significant shade contamination prior to solar noon. An SP1A spectralphotometer at COVE scans downward to observe upwelling radiances reflected by the sea, a boundary condition needed to improve the accuracy of satellite retrievals for both aerosols (i.e., Mishchenko and Travis, 1997) and clouds. The SP1A is stable over a wide dynanmical range (i.e., across the sun glint); it was purchased by GACP, which also analyzes the data, and is operated by CERES. GSFC installed an AERONET (Cimel) sunphotometer (Holben et al., 1998) on the ocean platform in October, 1999.

Figure 6 see next page **CERES Ocean Validation Experiment (COVE).**

CERES Ocean Validation Experiment (COVE)

Long term radiation measurements at a stable sea platform.
20 Km off the Coast at the Chesapeake Lighthouse.

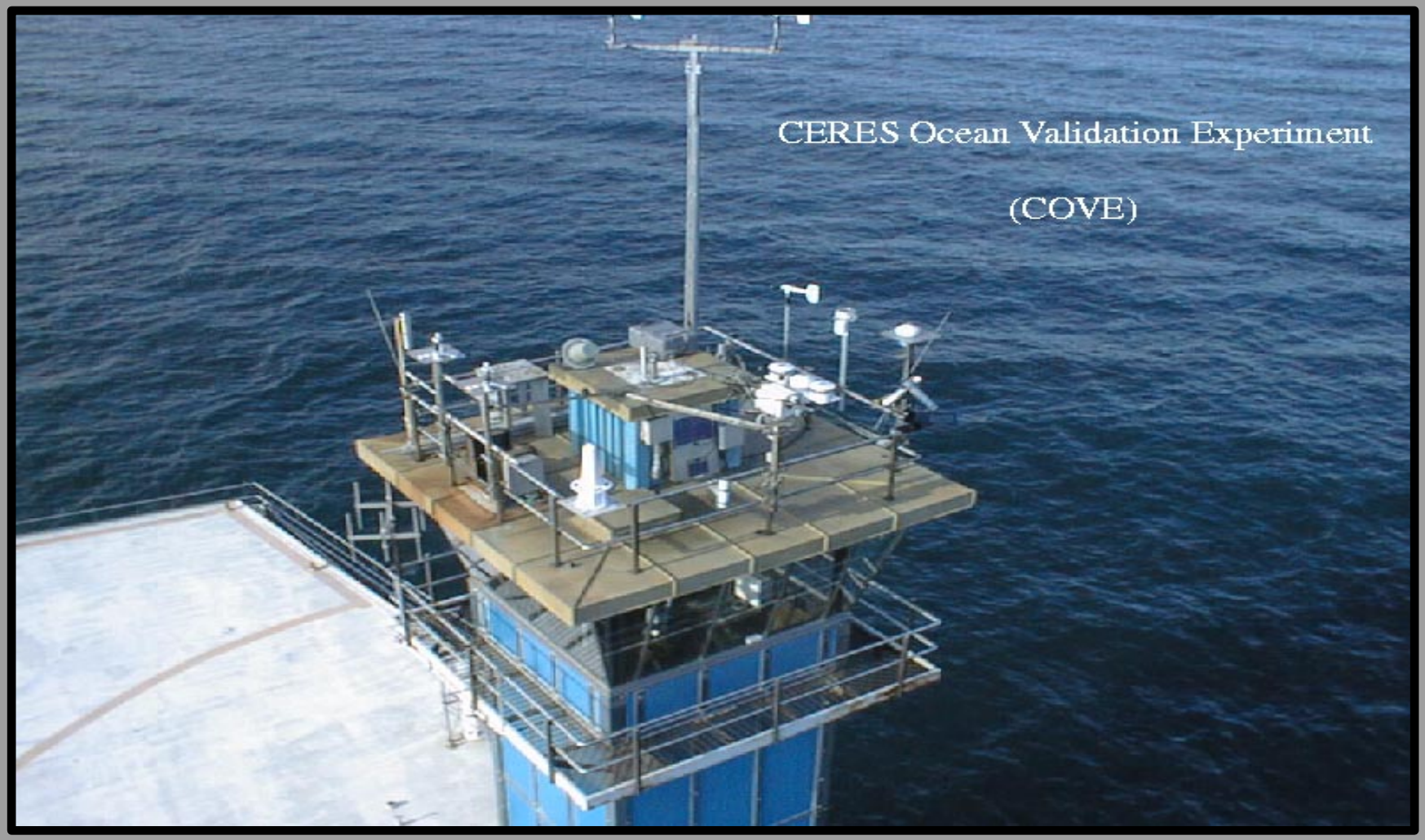

- Upward and Downward: Broadband Flux, Spectral, Directional Radiance
- Broadband (BSRN), MFRSR, Cimel (AERONET), SP1A (GACP), wave and meteorology (NOAA)
- Aircraft campaigns with C-FAR for spectral flux and BRDF

http://www-svg.larc.nasa.gov/~Ceres/data/index.html

One sampling problem that COVE will address relates to ocean albedo. SARB calculations assume an ocean spectral albedo and adjust the cloud (aerosol) properties in cloudy (clear) footprints to more closely match the CERES TOA observation. Does the classic distribution of sea slopes (Cox and Munk, 1954, 1955), presently in wide use to parameterize ocean optics as a function of surface wind speed, provide an adequate sampling of true sea slopes? Recent measurements of laser glitter (Shaw and Churnside, 1997) from the sea that have been applied to microwave remote sensing (Lin et al., 1999) indicate that sea slope also depends significantly on the temperature difference of the sea and air. In CERES, we presently use only a wind-speed dependent Cox-Munk with adjustments for aerosol and cloud optical depth, "underlight", and sea foam (white caps). Figure 7 (see next page) shows our predicted broadband albedo (red marks), using Yongxiang Hu's parameterization of Cox-Munk in spectral bands fitted to the Fu-Liou code, and based on observations of wind speeds, spectral AOT, and Long and Ackerman (2000) cloud screening at COVE. The observed sea albedos at COVE (black marks in Figure 7) are generally larger than the computed values for cosSZA less than 0.5. Are our theoretical albedos too small because of a large coastal "underlight" (particle reflection) at COVE? The Payne (1972) parameterization for broadband sea albedo, based on measurements in Buzzard's Bay, for atmospheric transmission 1.0 (0.6) is shown as a solid (dashed) line. Excess coastal underlight is indeed a possibility for COVE (20 km off Virginia Beach) or Buzzard's Bay (Massachusetts).

Figure 7 (see next page) **Ocean broadband albedo at COVE under clear skies. Observations (black plus). Lookup to theory using wind and AOT observations in 30-minute interval (red). Lookup to theory using wind in 30-minute interval and AOT observed during same day (blue). Fit to Payne (1972) results for transmission 1.0 (solid line) and 0.6 (dashed line).**

COVE Observed Afternoon Clear Sky Albedo (Black Plus)
Hu_Cox_Munk / Fu_liou Modeled Ocean Albedo (Red diamond)
Payne Trans=1.0(solid) Trans=0.6(dashed) Cloud:0.10

AOT,WIND,PW exist(red) AOT,PW not avail.(blue)

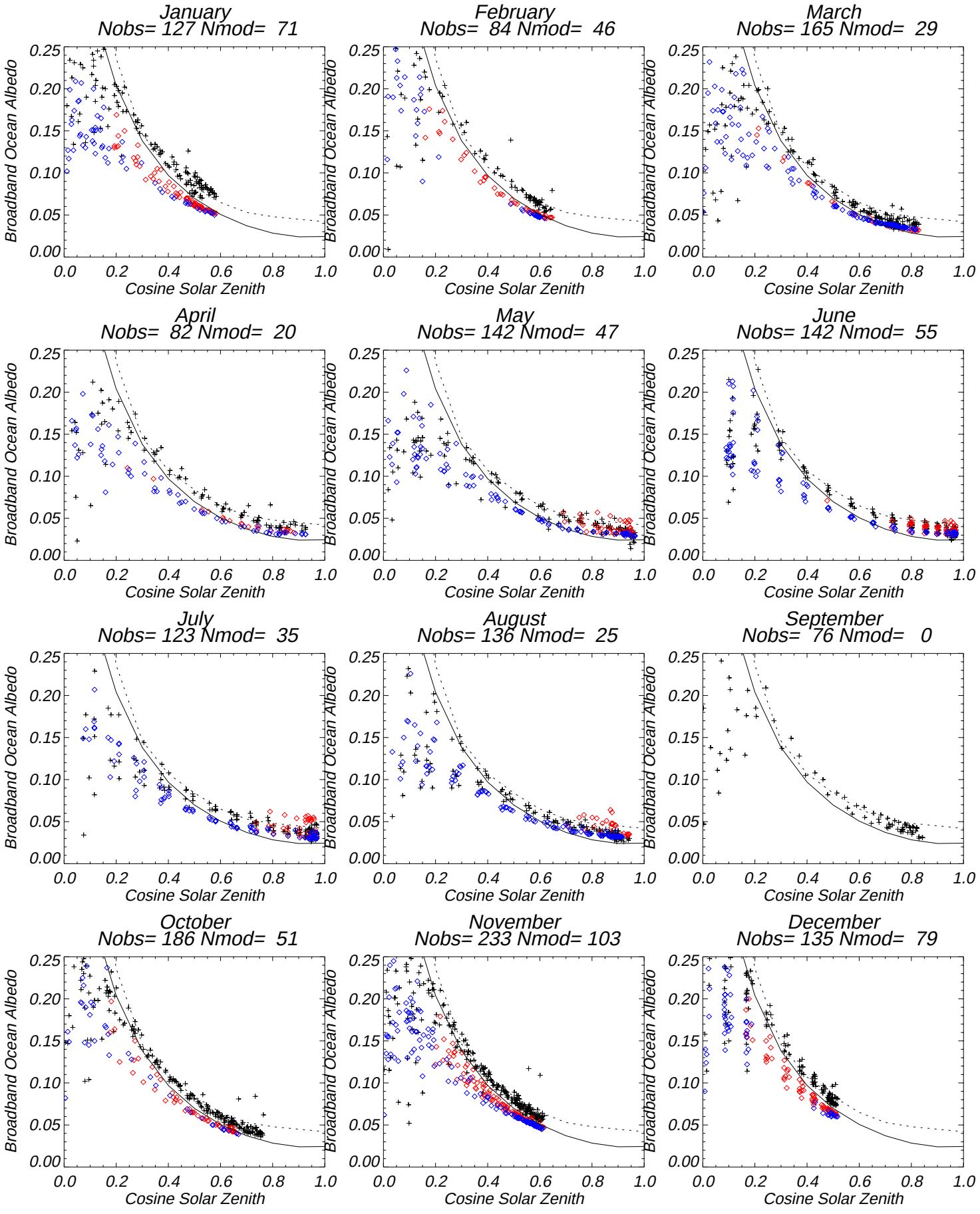

An improved parameterization of the ocean albedo and BRDF (i.e., an adjustment to the current formulations based on Cox-Munk) would advance retreivals of clouds by CERES and aerosols by GACP and EOS. We have deployed the downlooking SP1A at COVE - which has routine measurements of wind, wave structure (near IR rangefinder deployed ty NOAA), and spectral AOT as well as broadband fluxes - to build the database for such a parameterization. Because of coastal underlight, the COVE measurement in the visible portion of the spectrum are not completely representative of the open ocean. But COVE spectral measurements in the near-IR are not contaminated with underlight; in the near IR, the absorption by water is strong enough to ensure that only sea slope and surface foam make signficant contributions to the reflectance. Hence, an empirical parameterization for the effect of winds (affecting sea slope and foam) and air-sea temperature differences (affecting sea slope) on ocean spectral reflection in the near IR could be developed with data at COVE; and it would be representative of the open sea. We plan to do this, and then scale the results to account for wind and temperature into the visible. The parameterization should be a boon for ocean remote sensing generally; by then describing the effects of wind and temperature on sea optics as purely surface effects, a SeaWiFS observation could be used to infer the true ocean underlight. A later section will describe a Chesapeake Lighthouse and Aircraft Measurements for Satellites (CLAMS) field campaign. CLAMS will validate the parameterization and determine how spatially representative the COVE measurements are.

Surface monitoring sites for CERES validation are placed in 3 categories:

Class 1 "**Remote Sensing Physics**" sites will be used to test the physics of CERES remote sensing and radiative transfer with comprehensive descriptions of atmospheric and surface variables. The ARM Cloud and Radiation Testbed (CART) Southern Great Plains (SGP), North Slope of Alaska (NSA), and Tropical West Pacific (TWP) sites are in this category (see http://www.arm.gov/docs/sites.html). We place COVE in this category because of its unique ability to monitor the actual surface boundary conditions (spectral radiances upwelling from the sea and measured by SP1A) that are assumed by algorithms to retrieve aerosol and cloud properties; not even the ARM sites have such measurements of the surface. The instrument complement at the ARM central sites include unique collocations of active and passive cloud and aerosol sensors (i.e., Mace et al., 1998); these will be vital in assessing CERES estimates of factors such as cloud overlap and its impact to the radiation profile. Class 1 sites will be used primarily to improve the absolute accuracy of CERES products.

Class 2 "**Regional Climate Trend**" sites monitor a limited number of critical parameters. We will combine Class 2 site measurements with the satellite products to describe regional secular changes in the radiative forcing of clouds, the surface, and aerosols (i.e., aerosol forcing in Figure 4). Surface monitoring at all Class 2 sites must include meteorology, broadband SW and LW fluxes, and aerosol optical depth (i.e., the MFRSR of Harrison et al., 1994); these measurements are needed to confidently "subtract the atmosphere" with MISR, MODIS, ASTR, and CERES data. Other measurements are desirable; spectral SW, PAR, UVB, aerosol absorbing (physical and chemical) properties, cloud condensation nuclei, and cloud lidar (to 20 km, such as Spinhirne, 1993, MicroPulse Lidar), cloud radar, and passive microwave. If a secular trend is seen in the CERES retrievals, careful analysis with Class 2 time series with SARB radiative transfer will permit us to diagnose the approximate but distinct forcings of clouds, aerosols, ozone, and surface optics to that trend. Simultaneous, long-term measurement of multiple parameters is critical; they are needed to determine, for example, whether a weak trend in TOA reflection is due to an increase in thin cirrus contrails, a change in aerosol, or a change in the surface. This will enable us to quantify the current big mysteries in anthropogenic radiative forcing, namely regional changes in aerosols and land use. Experience with the modeling of climate perturbations from recent volcanic eruptions indicates that the signal of small changes to forcing can be detected and used quite effectively.

Class 3 "**Discrete Validation**" sites will be selected from those monitoring facilities with readily available and accurate measurements. Examples of Class 3 are those BSRN sites without aerosol photometers, the NOAA Integrated Surface Irradiance Study ISIS sites, and most of the Global Energy Balance Archive (GEBA) sites compiled by ETH in Zurich. Class 3 sites are essentially targets of opportunity that are established and run by other agencies.

We place special stress on Class 2 (Regional Climate Trend) sites because of the unique potential of these sites to enhance the ability of EOS to monitor particular radiative forcings to climate. Class 1 (Remote Sensing Physics) sites are rare. We are confident that sufficient numbers of Class 3 (Discrete Validation) sites will be in place internationally. EOS interest in Class 3 sites must build, however, if the individual site scientists are to obtain the resources needed to improve the accuracy and maintain the continuity of their measurements. EOS application of Class 2 Regional Climate Trend sites is absolutely critical. If we lack Class 2 Regional Climate Trend CO-LOCATED monitoring of surface radiative flux and aerosol optical properties, our EOS estimates of aerosol radiative forcing will be essentially unvalidated;

purported regional trends in surface albedo and many other EOS land products would be suspect to aerosol contamination. Large regional trends in aerosol loading are anticipated in the next few decades; clean up of industry in the U.S. and especially Eastern Europe; industrialization of China and Latin America; changing agriculture and biomass burning in South Asia, Africa, and Latin America. It is imperative that a global observing system be able to separate aerosol trends from surface trends. EOS should purchase supplementary monitoring instruments for Class 2 sites that have the expertise and will to properly operate and maintain them.

Continuous, daily data from all 3 categories of sites will be used for CERES SARB validation. Field campaigns that measure the vertical profiles of fluxes with aircraft are expected at the Class 1 sites. Field campaigns to measure surface optical properties from low altitude aircraft will be conducted at representative Class 1 and 2 sites. A subsequent section describes our Chesapeake Lighthouse and Aircraft Measurements for Satellites (CLAMS) field campaign scheduled for summer 2001. We have identified SURFRAD, CMDL, and several other BSRN sites as Class 2, rather than Class 3, largely because of our confidence that high quality, long-term, collocated monitoring of basic radiometric quantities will continue at these sites. CERES has purchased 4 MicroPulse Lidars (MPL) to measure cloud-base height and estimate the vertical distribution of aerosols at selected Class 2 sites; the first will be deployed at the Saudi Solar Village (see list of CAVE sites in subsequent section and Table 9); and all will be overseen by MPL-Net (http://virl.larc.nasa.gov/mpl-net/), which is directed by James D. Spinhirne at GSFC.

5.2.3 Measures of Success

The Suttles and Ohring (1986) survey of needs for the global SRB indicated that the desirable accuracies for surface SW and LW fluxes were +/- 20 Wm^{-2} for instantaneous and +/- 10 Wm^{-2} for a monthly average. The bias of surface SW flux in the current GEWEX SRB Project (Whitlock et al., 1995) exceeds 10 Wm^{-2}; this was achieved only after a thorough round of algorithm intercomparison and extensive validation with ERBE TOA and GEBA surface measurements. Table 6 estimates the absolute accuracy of present measurements of radiation at the surface, contrasting them with accuracy at the TOA, anthropogenic forcings, and possible trends in the planetary radiation budget:

Table 6

Accuracy of surface observations:
Baseline Radiation Network (BSRN) operations Manual
(WMO /TD-No. 879, 1998)
BSRN is a high quality standard to which the best stations may subscribe.

Quantity at surface	Capability	Goal
Direct solar irradiance	1% or 2 Wm-2	
Diffuse solar radiation	10 Wm-2	4% or 5 Wm-2
Global (SW) radiation	15 Wm-2	2% or 5 Wm-2
Reflected shortwave radiation	15 Wm-2	5%
Downwelling longwave radiation	30 Wm-2	5% or 10 Wm-2
Upwelling longwave radiation	30 Wm-2	5% or 10 Wm-2

Accuracy of TOA ERBE observations:
Global annual net (SW-LW) ~ 5 Wm-2
Regional monthly uncertainty ~ 6 Wm-2
Year-to-year fidelity (if continuous) ~ 1-2 Wm-2
(CERES better by factor of four)

IPCC 1995 Forcing:
Well-mixed anthropgenic gases +2.45 Wm-2
Direct aerosol at TOA –0.2 to –0.8 Wm-2
Indirect aerosol at TOA ~0.0 to –1.5 Wm-2

World Ocean heat storage:
From mid-1950s to mid-1990s “warming rate of 0.3 Wm-2”
(Levitus et al., 2000)

Geothermal heating:
~0.06 Wm-2 (Oort, 1992)

Table 7 (see next page) shows our target for the accuracy of the CERES SARB retrievals. The “bias” is here our estimate for the difference of a archived, constrained (tuned) product from the true flux. The rms error below is the total error (bias plus random) in the retrieval. Errors are given for CERES footprints as instantaneous for a typical daytime sun illumination and for 1 degree equal angle gridboxes as a monthly mean. The monthly mean has sun half of the time, so SW bias errors for footprints are twice the bias errors for gridboxes; we have optimistically assumed that in going to the monthly-averaged grid, the application of geostationary data has modeled the diurnal cycle perfectly. Table 7 estimates the absolute accuracy of a retreival; the precision (i.e., for monitoring long term trends) should be at least as good. These are global estimates; errors for some conditions (i.e., the SW reflected from the surface of a snowfield) will be larger.

Table 7 Bias:Rms error goals for constrained SARB fluxes

	bias:rms for fluxes (Wm-2)			
	Footprint Instantaneous (daytime sun)		**Gridded** (1x1) Monthly mean (24-hour clock)	
	Clear	All sky	Clear	All sky
Surface				
SW up	2:10	2:10	1:5	1:5
SW down	20:30	20:30	10:15	10:15
LW up	2:15	2:10	2:10	2:10
LW down	8:15	12:20	8:15	12:15
500 hPa				
SW up	5:30	10:30	2:10	5:10
SW down	20:30	20:30	10:15	10:15
LW up	8:15	12:20	8:12	12:15
LW down	8:15	12:20	8:12	12:15
200 or 70 hPa				
SW up	4:30	4:30	2:10	2:10
SW down	8:10	8:10	4:5	4:5
LW up	5:15	5:15	5:10	5:10
LW down	3:5	3:5	2:3	2:3
TOA				
SW up	3-4:30	3-4:30	2-3:10	2-3:10
LW up	1-2:15	1-2:20	1-2:10	1-2:10

5.3 Pre-launch algorithm test/development activities

5.3.1 Field Experiments and Studies

The cooperative CERES/ARM/GEWEX Experiment (CAGEX) has been our primary contribution to pre-launch validation using field campaign data. As noted earlier, CAGEX is a public access set of input data, calculated fluxes, and validating measurements over the Department of Energy Atmospheric Radiation Measurement (ARM; Stokes and Schwarz, 1994) Southern Great Plains (SGP) Cloud and Radiation Testbed (CART) site in Oklahoma, U.S.A. Version 1 of CAGEX uses a 3 by 3 grid (0.3 deg on each edge) every 30 minutes from 1409 UTC to 2239 UTC (daylight) for 26 days, starting on April 5, 1994. CAGEX Version 1 now provides on-line access (see http://snowdog.larc.nasa.gov:8081/cagex.html) to:

(1) satellite-based cloud properties and atmospheric sounding data that are sufficient for broadband radiative transfer calculations;
(2) vertical profiles of radiative fluxes calculated with that data as input; and
(3) validating measurements for broadband radiative fluxes and cloud properties.
Version 2.2.0 includes (1), (2), and (3) for the 38-day ARM Enhanced Shortwave Radiation Experiment (ARESE), 25 September to 1 November, 1995. GOES cloud retreivals and estimates of broadband TOA fluxes (Minnis et al., 1995) are a cornerstone of CAGEX. The documentation and on-line plotting features of Version 2.2.0 are especially user-friendly. For any selected day of ARESE, CAGEX Version 2.0.0 offers a plethora of time series and difference plots for (1), (2), and (3) on demand. For the 38-day mean, differences of computed and observed fluxes are presented using various inputs for the Fu-Liou code. Table 8 (see next page) shows biases (calculations minus observations)for broadband LW using core radiosonde inputs and various perturbations to the humidity profile. In Column E, the Eta mesoscale model Data Assimilation System (EDAS; Yarosh et al., 1996) has been used for the temperature and humidity inputs; this is a rough analog to the global ECMWF used in CERES. Other sources of humidity include AERI (temperature and humidity profiles inverted from a longwave Fourier Transform Spectrometer), the Microwave Radiometer (MWR was used to scale the radiosonde PW), and the Global Positioning System (GPS retrievals of PW were used to scale the radiosonde PW).

Table 8 LW (computed – observed) in CAGEX Version 2.2.0

Fall 1995 at ARM SGP in 30-minute intervals

computed-observed (Wm-2)	full-sky humidity sensitivity							
	A	B	C	D	E	F	G	H
OLR	2	-9	11	0	1	3	2	2
Surface net LW	-3	26	-24	0	-6	-2	-1	-4
Surface up ULF	-2	-2	-3	-2	-2	-2	-2	-2
Surface down DLF	-6	24	-27	-3	-8	-4	-4	-7

computed-observed (Wm-2)	clear-sky humidity sensitivity							
	A	B	C	D	E	F	G	H
OLR	4	-8	13	1	1	3	3	3
Surface net LW	-4	28	-25	0	-8	-4	-4	-5
Surface up ULF	-2	-2	-3	-2	-2	-2	-2	-2
Surface down DLF	-6	26	-28	-3	-10	-7	-7	-7

Column A - Calculations use core (radiosonde) input data.
Column B - Core input, doubled humidity.
Column C - Humidity is half that of the core input.
Column D - Core sounding data, with humidity added
10% added to the humidity from surface to 700 mb.
20% added to the humidity from 700 mb to 500 mb.
30% added to the humidity from 500 mb to 250 mb.
Column E - Eta sounding dataset used.
Column F - AERI sounding dataset used.
Column G - MWR sounding dataset used.
Column H - GPS sounding dataset used.

Recall that the observed broadband fluxes at TOA are estimates from narrowband GOES-8 window measurements, with additional assumptions for sensor calibration and angular distribution modeling (ADM; conversion of radiance to flux). Table 6 gives a pessimistic assessment for the accuracy of the broadband PIR measurement of downward longwave flux (DLF) at the surface. The clear-sky matrix in the middle shows that for Column A (radiosonde humidity profile), the time-mean computed DLF is 6 Wm-2 less than the observed mean. Should the reader click on the "-6" in Table 8 in CAGEX Version 2.2.0 while on-line,the scatterplot of Figure 8 (see next page) will immediately appear.

Figure 8 (see next page) **Measured and computed DLF in CAGEX Version 2.2.0. Fall 1995 at ARM SGP in 30-minute intervals.**

Surface Downwelling Longwave Flux

Fu-Liou vs Pyrgeometer
Core input
Core aerosols
SIROS radiometry

October 1995 ARESE — CAGEX central grid

	Full-Sky	Clear-Sky	Cloudy-Sky
Fu-Liou mean	318	297	343
Measured mean	324	303	348
Bias	-6	-6	-6
% Error	-2	-2	-2
% Error std. dev.	7	3	7
Samples	1209	551	466

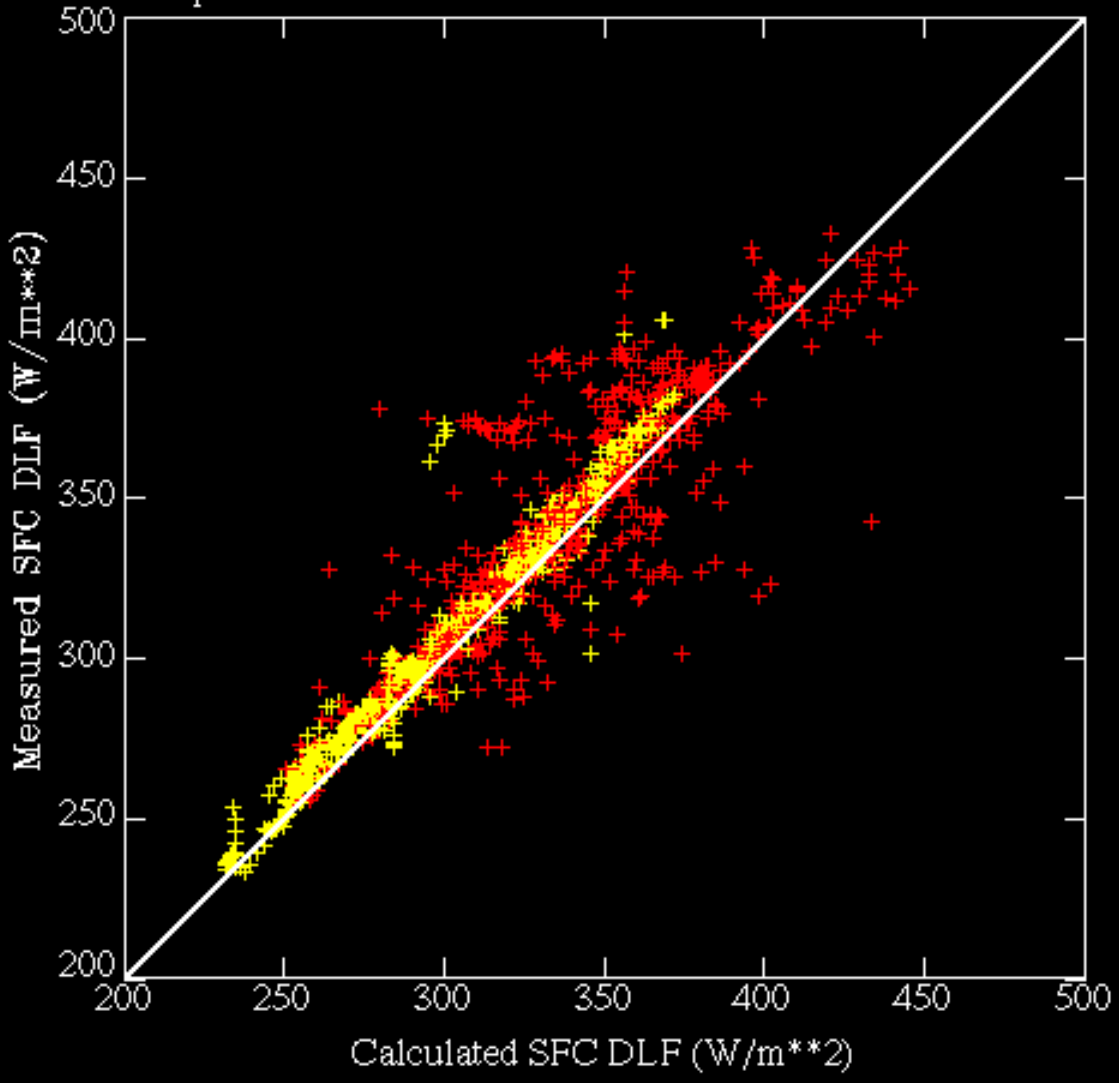

CAGEX Version 2.2.0 (Charlock and Alberta, 1999)

Clough (personal communication) reports that the Rapid Radiative Transfer Model (RRTMl; Mlawer et al., 1997) used in the ARM Quality Measurement Experiment (QME) has a similar bias for clear skies as the Fu-Liou code in Figure 8. The full-sky bias (-6 Wm-2) is remarkably small in Figure 8, considering the huge scatter. It suggests that the cloud geometrical thickness inferred by Minnis et al. (1995) is sound for the time mean. CERES uses a more advanced cloud retrieval from the same group. CAGEX Version 2.2.0 includes a comparison of the GOES-8 cloud base heights to a ground-based cloud profiling radar (CPR) mentored by Eugene Cloithaux and lidar (Spinhirne et al., 1993). Tests of the Fu-Liou code with CAGEX (Charlock et al., 1998) and with other SGP data (Fu et al., 1998) have led to improvements and more sophisticated treatements of aerosol inputs (Hess et al., 1998, Tegen and Lacis, 1996).

The CERES ARM Radiation Experiment (CARE) field campaign was held at SGP during August 1998 to measure the surface SW broadband albedo, SW spectral bidirectional reflectance, and the angular dependence of LW window radiance with a helicopter (i.e., Whitlock et al., 1994). An improved spectrometer surveyed 0.35-2.5 micron in 0.01 micron steps over 6 surfaces: grass, milo, soybeans, fallow wheat (a burned wheat stubble with the appearance of brown dirt), and alfalfa. Each surface was observed at 4 solar zenith angles (SZA).

CAGEX algorithms used simplified surface optical properties based on Briegleb et al. (1986) which are maintained as on-line maps (http://tanalo.larc.nasa.gov:8080/surf_htmls/SARB_surf.html). For some surface types, CARE provided advances to optical property inputs for global scale SARB calculations with the Fu-Liou code (Figure 9 see next page). Other CARE measurements by DOE provided a higher degree of closure on SW calculations in clear skies (i.e., Kato et al, 1999 and previous section 5.2.2.4). Yaping Zhou has reduced the helicopter measurements at 300m to represent actual surface reflected spectral radiances (i.e., Figure 10, wherein the sun is at the left); note that the wavelength dependence of Rayleigh and aerosol scattering has yielded a much stronger “correction” at 400 nm than at 900 nm. We will use the detailed observations over these surfaces, and subsequent measurements with the CERES OV-10 fixed wing aircraft, to interpret MODIS global surveys of land type and BRDF classes by MODIS in radiative transfer calculations.

Figure 9 (see next page) **Spectral albedo over grass from August 1998 CARE in Oklahoma**

Figure 10 (yet another page) **Reflected radiances at 400 nm and 900 nm over grass at SZA=45 deg. Helicopter @ 300m (top) and adjustments to surface (bottom). August 1998 CARE**

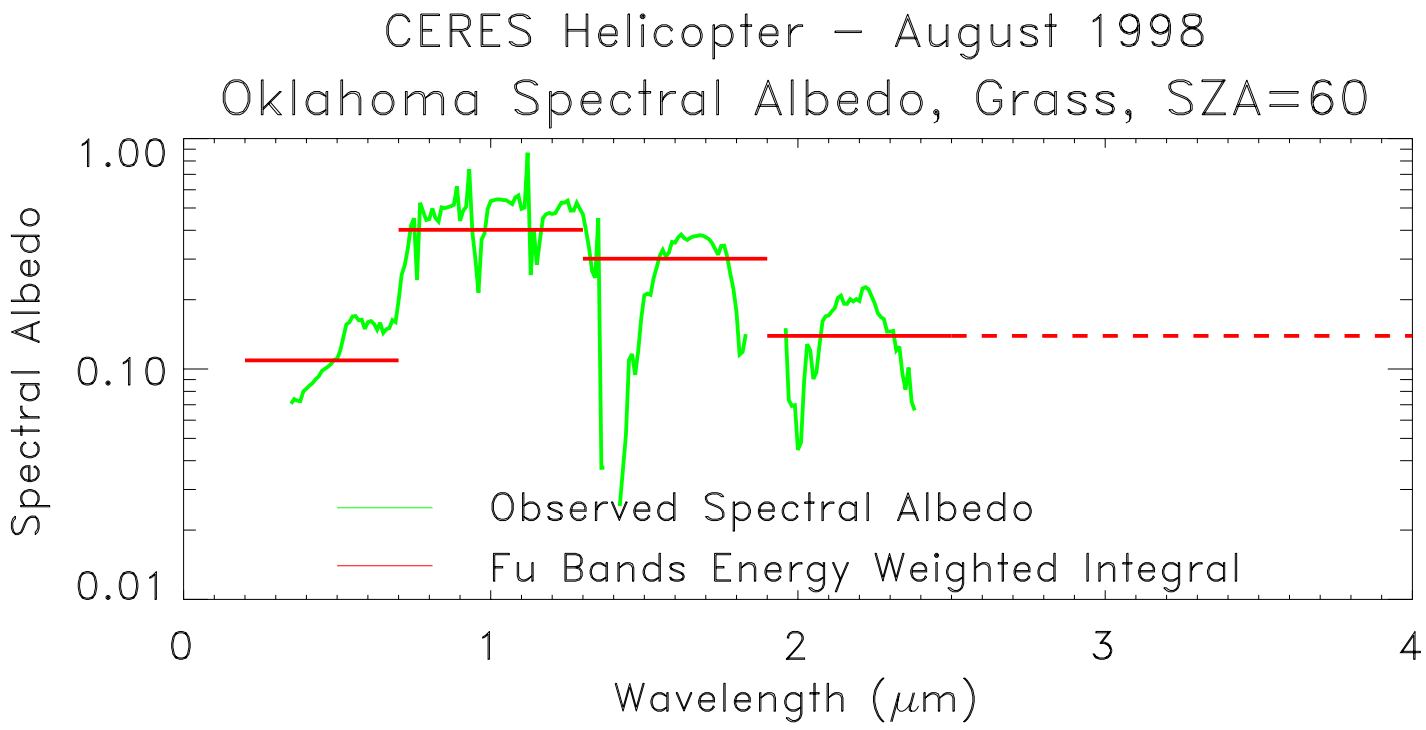

Global maps for reference surface optics:
http://tanalo.larc.nasa.gov:8080/surf_htmls/SARB_surf.html

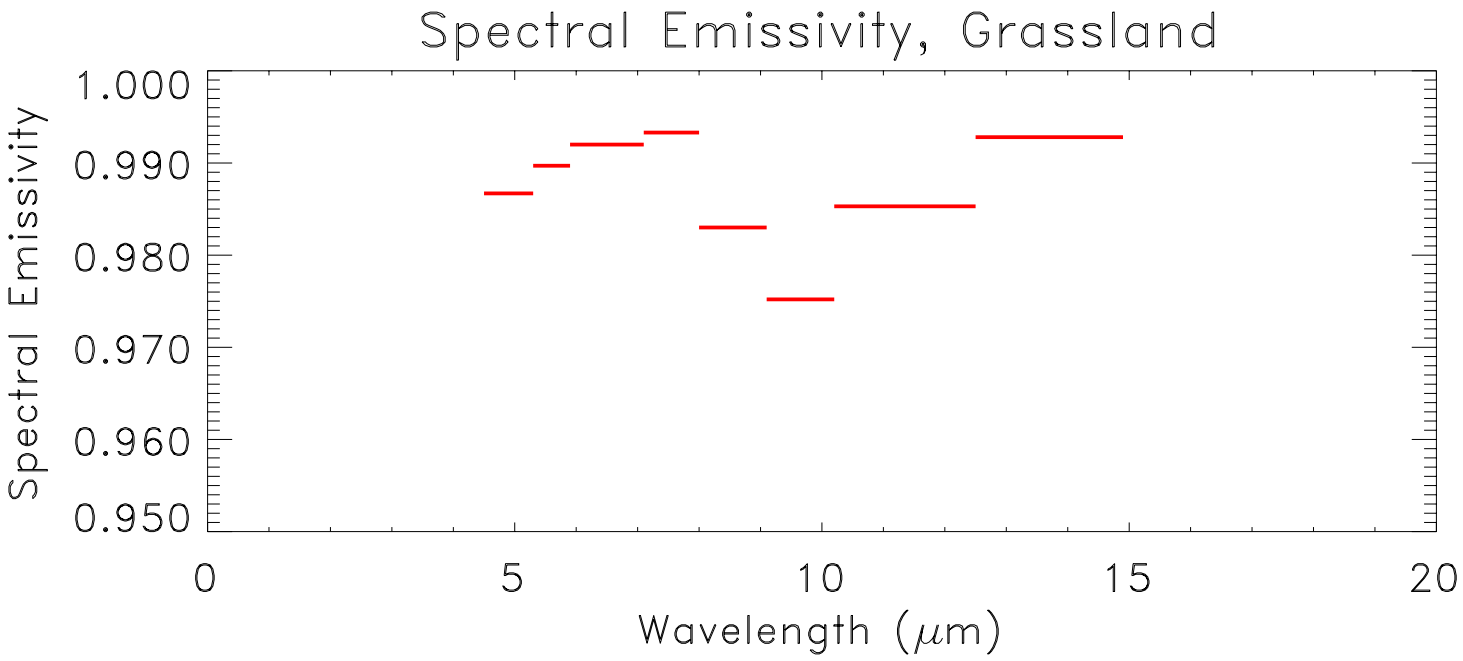

CERES ARM Radiation Experiment (CARE)
Oklahoma August 98

HELICOPTER (300m)

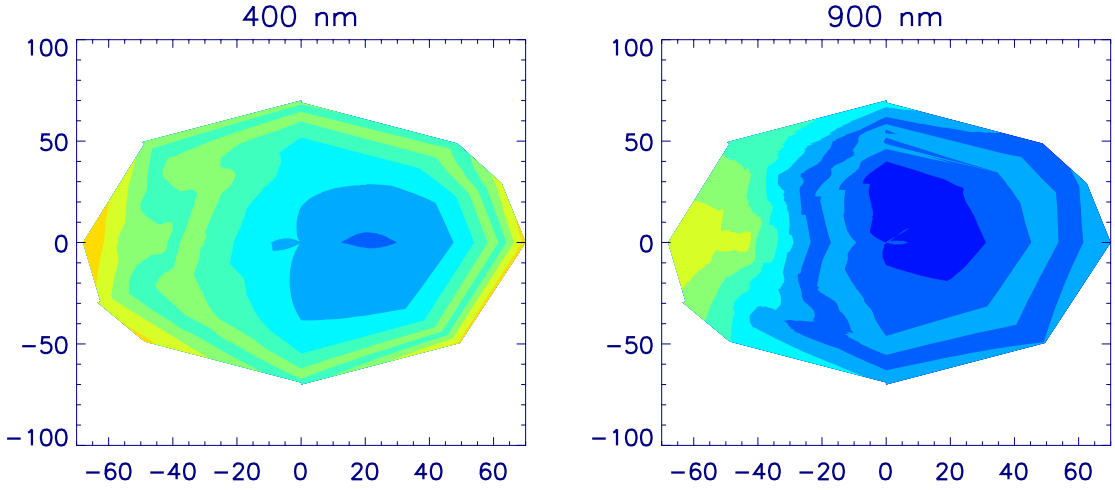

ADJUSTED TO SURFACE (0m)

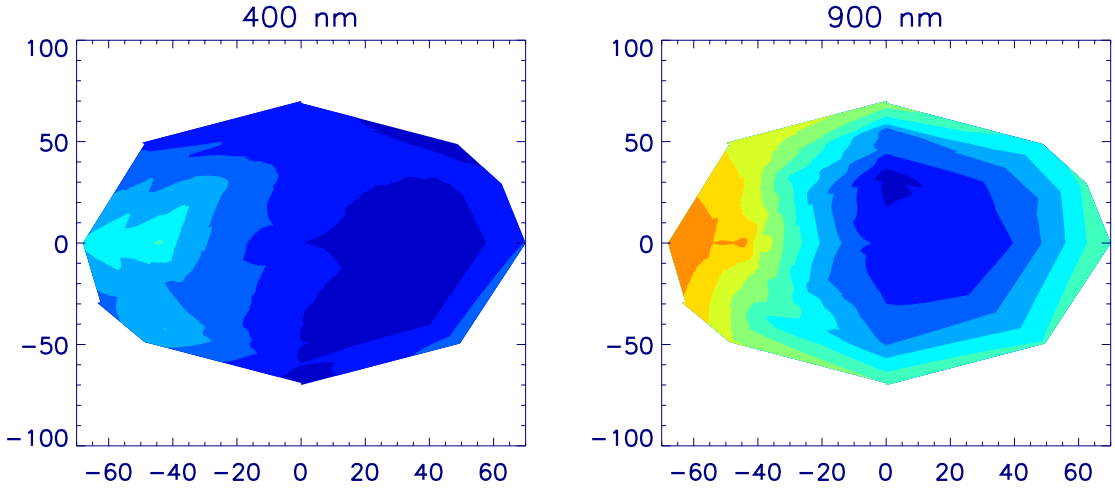

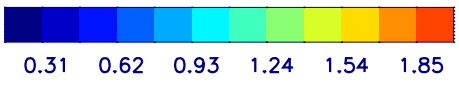

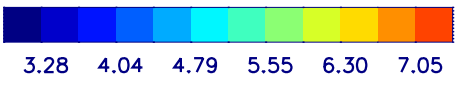

SCENE: GRASS SZA = 45

5.3.2 Operational Surface Networks and Existing Global Satellite Data

The on-line CAVE (http://www-cave.larc.nasa.gov/cave/) is our primary vehicle for utilizing the measurements made by others to validate the SARB component of CERES. CAVE interacts with the SURFRAD and CMDL teams that are supported by EOS validation funds, as well as with other organizations in the radiation observation community such as ARM and BSRN. Data is reformatted in CAVE and value is added. For example, the first order corrections for thermal offset on CAVE now provide the ARM community with the most accurate form of their own broadband surface record. CERES data is collocated and subset at CAVE for convenient use (Figure 11 see next page).

CAVE is structured in continuous, half-hourly time blocks. To form a daily mean, the analyst simply sums 48 half-hour blocks. When provided, the CERES TOA data is instantaneous at the footprint level; the record now contains TRMM ES8. Each site now on-line (see Table 9, which is yet another page after Figure 11) contains data on surface broadband radiation and surface meteorology. Many sites include a record of spectral AOT. Our goal is the development of a continuous record of these variables, starting January 1, 1998.

CAVE also has on-line files of atmospheric temperature and humidity at a few sites for limited time periods. CIMSS (Feltz et al., 1998) has furnished soundings based on longwave spectral measurements (GOES at TOA and AERI at the surface) at the ARM SGP Central Facility. Some EDAS and GEOS 2.0 profiles (both NWP analyses) are available thru CAVE for the SGP. John Augustine has furnished soundings for the SURFRAD sites based on interpolations of radiosonde data.

As CERES advances, we will take a closer look at products such as the aerosol size distributions and single scattering albedos that are retrieved by AERONET. More sophisticated information on the optical properties of the surfaces around the CAVE sites will be added later (i.e., as we obtain OV-10 and MISR data). Another focus will be on upper tropospheric humidity UTH (Soden et al., 1994). Within-atmosphere fluxes from aircraft will eventually be included in CAVE.

Figure 11 (see next page) **Map of sites where CAVE data is now collected**

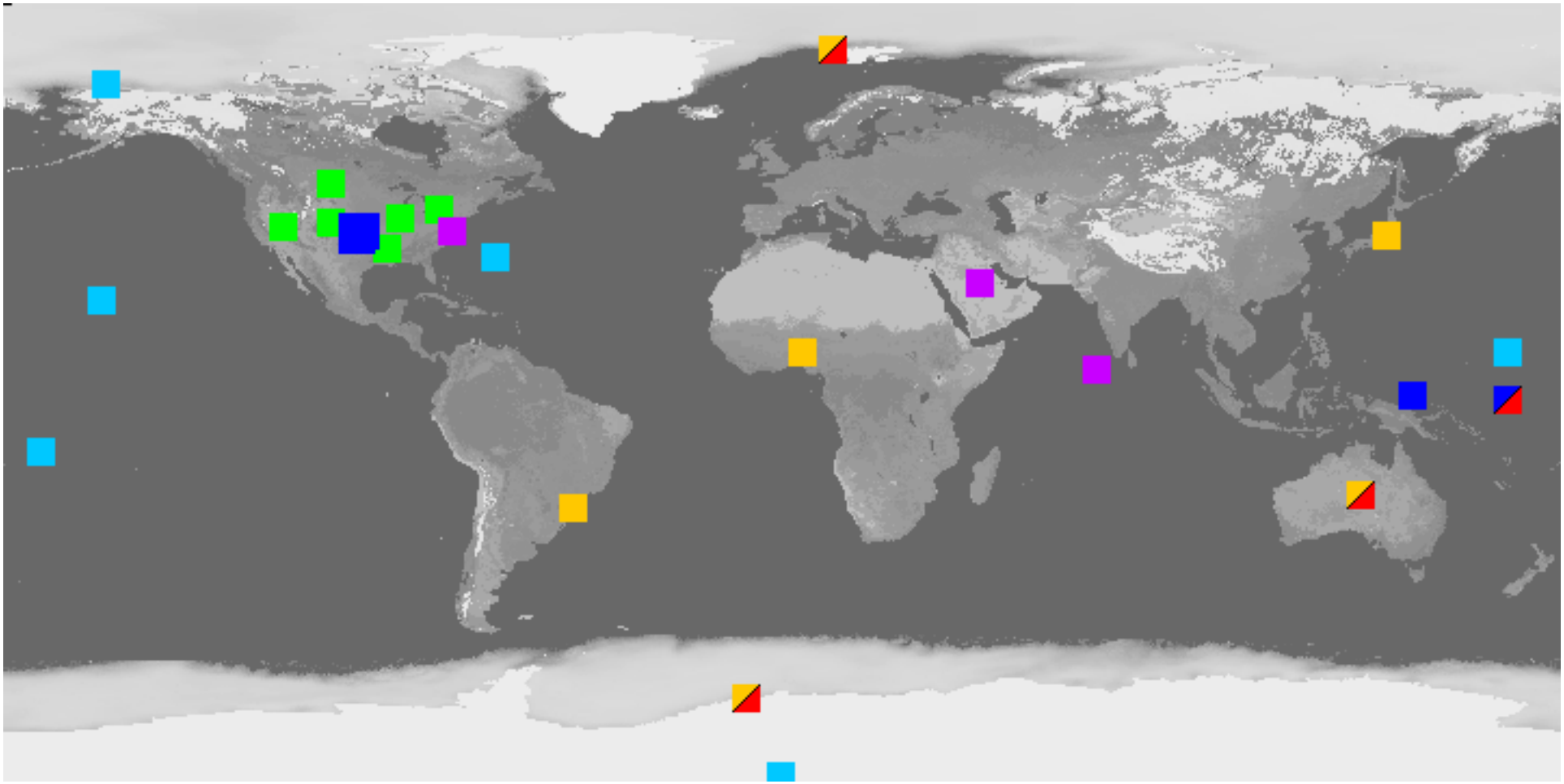

Table 9 CAVE sites now on-line (and used in Figures 13,15)

BSRN		ARM SGP	
	Alice Springs, Australia		Larned
	Florianopolis, Brazil		Hillsboro
	Georg Van Neumayer, Antarctica		LeRoy
*1	Ilorin, Nigeria		Plevna
	Ny Alesund, Spitzbergen		Halstead
	Tatano, Japan		Towanda
			Elk Falls
CMDL *2			Coldwater
	Barrow, Alaska		Ashton
	Bermuda		Tyro
	Boulder, Colorado		Byron
	Kwajalein Island		Powhuska
	Mauna Loa, Hawaii		Lamont
	Samoa		Ringwood
	South Pole		Vici EF
			Morris
	Kaashidhoo Island, Maldives		Meeker
			Cordell
*6	COVE (Chesapeake Lighthouse)		Cyril
			Seminole
*3	Saudi (Arabia) Solar Village *5	*6	Central Facility
SURFRAD *4		ARM TWP	
	Bondville, Illinois		Manus
	Boulder, Colorado		Nauru
	Desert Rock, Montana		
	Fort Peck, Montana		
	Goodwin Creek, Mississippi		
	Penn State, Pennsylvania		

*1 Pinker Validation PI
*2 Dutton Validation PI (also help on PSP thermal offset)
*3 Myers Validation PI
*4 Augustine Validation PI (also Long-Ackerman software)
*5 Spinhirne MPL-net coming
*6 AERONET advises CERES about site

The CAVE on-line record is presently missing a few key sites (for example, ARM NSA, which is therefore not listed in Table 9). The total number of sites will increase, but probably not nore than by 50%. To be included in CAVE, a continuous record of high quality broadband fluxes (that we are permitted to distribute on-line) must be available.

5.4 Post-launch Activities

5.4.1 Planned Field Activities and Studies

The CERES-Fixed Wing Airborne Radiometer (C-FAR) on the low-level OV-10 aircraft (Figure 12 see next page) will be an important tool for CERES participation in EOS field campaigns. Section 5.2.2 on Sampling Requirements explained the need for measurements of surface optical properties in the vicinity of EOS validation sites. The C-FAR instrument complement on is based on the helicopter-based package used in the August 1998 CARE in Olkahoma (Figure 9). The FRS SW spectrometers look both up AND down, as do the broadband PSP pyranometr (SW) and PIR pyrgeometer (SW); these are observations of the components of net flux (LW). Meteorological sensors enable the OV-10 to serve as a low altitude sounder of temperature and humidity. Skin temperature can be obtained from 10-12 micron window measurements by the Heimann pyrometer.

The OV-10 has a much longer range than a helicopter; it can be readily deployed in support of validation activities by other EOS teams. In colloboration with MISR, the C-FAR was used in March 2000 to survey ocean spectral albedo in the vicinity of COVE. Seasonal effluent from the Chesapeake Bay estuary during April, May, and June each year flows toward the COVE platform, rendering the surrounding waters as “highly coastal”. The northern component of the estuary plume was measured by C-FAR during March 2000, but it had clearly not extended to COVE by that date.

Figure 12 (see next page) **OV-10 aircraft with CERES Fixed-wing Airborne Radiometer (CFAR)**

Fixed-Wing Airborne Radiometer

CFAR MeasurementComplement

UpLookingRadiometers

FRSpectralHemispheric0.42.20 µm
EppleyPSP0.33.0 µm
EppleyPIR550 µm

AmbientTotal Temperature
BarometricPressure

AmbientDewpoint Temperature
GPSPosition&Time
InternalFlightPattern Generation&
Navigation

GyroAttitudeand Heading

DownLookingRadiometers

FRSpectralHemispheric0.42.20 µm
EppleyPSP0.33.0 µm
EppleyPIR550 µm
NarrowFOVSpectralDirectionalRadiance Scanner0.352.5 µm(October2000)

5.4.1.1 Chesapeake Lighthouse and Aircraft Measurements for Satellites (CLAMS)

CLAMS is a aircraft field campaign that is planned for summer and fall 2001 at the CERES Ocean Validation Experiment (COVE) site – a rigid sea platform 20 km east of Virginia Beach. CLAMS is a clear-sky, shortwave (SW) closure campaign sponsored by CERES, MISR, MODIS-Atmospheres, and GACP. It seeks more accurate

a. broadband fluxes at sea surface and within atmosphere;
b. space-time variability for aspects of the ocean spectral BRDF;
c. retrievals of aerosols and radiative impacts with satellites.

using flights clear conditions (cloud-free but not aerosol-free). CERES, MISR (Terra), MODIS-Atmospheres, and GACP sponsor CLAMS. Besides the continuous, long-term COVE measurements, CLAMS will have flights by the NASA ER-2 (Air MISR, MAS, CPL, and possibly other instruments) and the Langley low-level OV-10 (broadband and spectral fluxes, spectral BRDF) aircraft coincident with Terra (~1030 LT). MODIS-Atmospheres plans 20 hours of ER-2 flying; MISR plans on 12 hours ER-2. Participtation by the University of Washington mid-level CV-580 (in situ aerosols and chemistry) is very likely. The French are considering deployment of the M-20 with an airborne POLDER and LEANDRE (lidar). CERES and Ralph Kahn of MISR collaborated to develop the CLAMS concept.

Sponsorship of the AIRS, as well as CERES, on Aqua will be sought for a second CLAMS during 2002. Highly accurate instruments for humidity sounding such as LASE DAIL (on DC-8) and the NAST-I (LW spectrometer) and NAST-MTS (microwave sounder) on Proteus will be sought.

The Langley OV-10 will be the workhorse of the summer 2001 CLAMS, flying at least one mission at low levels coincidently with every mission by any other participating aircraft. This will ensure that information from all flights can be interpreted in terms of net broadband flux, surface BRDF, and skin temperature. The other aircraft will seek clear sky missions coinciding with the morning overpass of Terra. The OV-10 will also fly at other times. In part to survey sea optics for a variety of solar zenith angles with the OV-10, CLAMS was planned to be near the summer solstice. A few flights will measure the profile of broadband (SW and LW) and spectral (SW) fluxes, upwelling and downwelling, in the boundary layer.

CLAMS is needed to fill gaps in SARB validation using COVE. There are two main limitations to the observations of broadband upwelling radiation at COVE. First, the platform obstructs some of the view of the ocean surface. Second, there are uncertainties in how well the ocean close to the platform (with or without obstruction) represents the sea in general. On the larger 20 km scale of a broadband CERES footprint, there are certainly systematic

variations in spectral albedo near COVE, which is 20 km off Virginia Beach. MODIS pixels will be used to scale the COVE sea optics to the larger CERES footprint. But does the sea bottom directly under the platform permit COVE measurements to adequately represent the sea within 1 km (the scale of an imager pixel like MODIS)?

The two issues can be resolved by a survey of broadband flux (up and down for SW and LW), downwelling spectral irradiance, and upwelling spectral irradiance and directional radiance with the CERES Fixed wing Airborne Radiometer (C-FAR) on the low-level OV-10 aircraft. In the months leading up to CLAMS, COVE will have measured the broadband upwelling fluxes (BSRN) and selected SW spectral radiances (SP1-A spectralphotometer) to establish the variations of albedo and BRDF for a wide range of conditions; sun angle, aerosol optical depth, cloud conditions, wind waves, large scale sea swell, foam, and particle loading within the sea. CLAMS flights of C-FAR will provide the needed offsets (due to platform obstruction) for a small subset of the huge sample gleaned from continuous COVE observations. And by exhaustively covering a few MODIS pixels, CLAMS will permit us to securely “scale-up” MODIS-based sea optics to the larger CERES footprint. MISR Validation has similar concerns about scene variability within its instrument’s FOVs (i.e., Kahn et al., 2000) and plans to use AirMISR on the ER-2, as well as C-FAR on the OV-10.

The variation the spectral SW radiance between imager pixels (MODIS, MISR, AVHRR, or SeaWiFs) nearby COVE under clear conditions is due, in turn, to spatial variations in both the optics of the sea and the aerosols above it; CLAMS will target both. A particular imager pixel centered on 1 km**2 may be adequeately surveyed near the sea surface by the OV-10; but because the imager views at an angle, aerosols at horizontal distances much greater than 1 km will affect the radiance to the satellite. An accurate “atmospheric correction” to a SeaWifs retrieval, for example, depends on aerosols spread over a larger area than just a single pixel projected to the sea surface. A separation of the spatial variation of aerosol loading from that due to ocean optics is needed to validate accurate retrievals of both quantities. This is especially the case if one seeks to retrieve the low “backround” loading of aerosols that force global climate. The CPL on the ER-2 will be the principal tool in CLAMS for determining the spatial variation of aerosols. Thin vertical “pencil” slices by CPL will be interpreted by MAS and AirMISR images from the ER-2. They will also serve as a testbed for developing algorithms of PICASSO-CENA. If the LASE on DC-8 is available, its flight may not coincide with the ER-2; a separate OV-10 mission would then be used to exploit the LASE description of the distribution of aerosols in space.

In situ aerosol and chemistry measurements by the CV-580 would provide CLAMS with an even higher level of

closure for aerosol optical properties. When combined with the CPL on ER-2 and the COVE surface-based instruments, there would be a description of the optical properties sufficient for rigorous testing of the physical assumptions on aerosols used in the retrievals of MODIS, MISR, GACP and CERES; and for a study of the CERES broadband ADM with radiative transfer calculations based on sound inputs. The vertical profiles of SW retrieved by SARB are strongly influenced by the profiles of aerosol absorption, which can be measured by the CV-580. Aerosol absorption is the principle source of decoupling between aerosol forcing at TOA and at the surface. INDOEX (Sateesh et al., 1999) found that surface and TOA forcing differed by roughly a factor of three; as hypothetical aerosol forcing may be vanishing at TOA but even exceed the forcing of anthropogenic greenhouse gases to the atmosphere itself, this has enormous implications for the global hydcrological cycle. CLAMS should be an excellent database for studies of aerosol assimilation (i.e., Collins et al., 2000, Rasch et al., 2000), which rely heavily on the retrievals of aerosol over the oceans.

Additional flights during fall 2001 are sought to meet the special needs of MISR. MISR requires especially stringent cloud free conditions (which may not coincide with the MISR week-long viewing cycle) and prefers low aerosol loadings for validation. The mean aerosol optical depth at COVE in July is about 0.3, which is suitable for MODIS aerosol validation. But the conditions required by MISR for coincidence of ER-2 (with AirMISR) and Terra may not be obtained in a single month (i.e., July 2001). If additional flights are needed for MISR (which will deliver the ER-2 with AirMISR), CERES will attempt to support these with low-level OV-10 flights as resources allow.

A second component of CLAMS in fall 2002 would permit CERES to validate the retrieval of the vertical profile of LW SARB by collaborating with AIRS in checking the vertical profile of water vapor (especially UTH) with NAST-I; NAST-MTS on Proteus with the AERI LW spectrometer at the COVE platform, and possibly an airborne LASE on the NASA DC-8 (August-September 2001). The LASE DIAL is probably the most accurate instrument for the measurement of UTH, which is the critical variable in the computation of the LW SARB profile. LASE on DC-8 can view up of down, profiling aerosols in addition to water vapor; it would be valuable for both SW and LW validation of CERES SARB and for SW investigations by the MISR (Aqua) team. NAST-I radiances on Proteus, which can operate efficiently at a wide range of altitude, would allow a spectral validation of the broadband LW SARB vertical profiles. In a second CLAMS, CERES OV-10 flights would measure the spatial variations SW sea optics for MISR and spatial variations of ocean skin temperature for AIRS. Such observations of ocean skin temperature and the humidity profiles would provide an ideal input for a theoretical similation of CERES LW TOA

radiances and fluxes under clear conditions. Comparably accurate input data would be much more difficult to obtain over land, where surface LW emission varies greatly in space due to canopy orientation, soil moiture and type, and viewing angle relative to the sun (Minnis et al, 2000 and Lin et al. 2000). Updated information on CLAMS is maintained at the URL www-cave.larc.nasa.gov/cave/ by clicking "CLAMS".

5.4.1.2 C-FAR Aircraft Surveys of Validation Sites

The C-FAR package on the OV-10 is currently being reconfigured to enhance the ability to measurement SW directional radiance. Between now and the summer 2001 CLAMS, we anticipate surveys of surface optical properties with C-FAR over a few area in Eastern North America. An early target includes the region of Canada between Great Lakes and James Bay during winter 2000-2001. This area contains snow and forest. The target is the albedo of snow and evergreen forest (typical albedo 0.3-0.4) versus snow and cropland (albedo then 0.7-0.8). This is the sharpest regular space-time variation in albedo that has an impact on daily weather forecasting, as demonstrated in studies with ECMWF. The goals are validation of CERES-MODIS-AVHRR surface albedo (i.e., Rutan and Charlock, 1997, 1999) and application by NWP. Flights will survey the natural combination of clear and cloudy skies over snow. During the past two decades, the seasonal snow cover in the NH has decreased by 10%; there is a need to quantify such effects (and validate them) in terms of energy (Wm-2).

5.4.1.3 ACE-Asia

CERES will participate in the Asian-Pacific Regional Aerosol Characterization Experiment (ACE-Asia) cooperatively with the NASA Langley component of GACP (http://www-cave.larc.nasa.gov/gacp/), which plans to send a postdoctoral researcher (Wenying Su) on the March-April 2001 cruise of the RV Ron Brown from Hawaii to Japan. The instrumentation to measure ocean optical properties on the RV Brown will be supplemented with observations of reflected radiances in channels from 350-1050 nm with the SP1A. A longer record from a duplicate SP1A is made at COVE. When coupled with other observations RV Brown (i.e., wind, spectral AOT), we will have the database with which to transfer the more extensive COVE observations to the open ocean. The SP1A observations from the RV Brown will be a test of our developing parameterization for selected channels of ocean BRDF. We will then have the ocean boundary conditions for a physcially based adjustment of AOT retrieved by MODIS, MISR, AVHRR, and the AOT produced by SARB constrainmentt; in addition to a direct check of the retrieved AOT with ship-borne photometers. Other comprehensive aircraft and ground-based measurements in

ACE-Asia will be useful for testing of the new generation of aerosol assimilations.

5.4.1.4 Ultra Long Duration Balloon (ULDB)

The Ultra Long Duration Balloon (ULDB) Project, managed by the Goddard Space Flight Center, is a balloon system capable of providing scientific measurements above 99% of the atmosphere. The balloons are scheduled for 100-day missions,launched from Alice Springs, Australia to an altitude of about 35km and transported by stratospheric winds around the globe while remaining between 15 and 50 deg of latitude South. The balloons are 200 meters in diameter and can carry payloads up to 1500kg. The main scientific goal of each mission can vary, but all the balloons will carry a set of pyrgeometers and pyranometers to monitor the shortwave (SW) and longwave (LW) radiation incident upon the balloon. CERES will use these flight opportunities to gather science-level broadband solar radiation data from the downlooking pyranometer. The accuracy of the pyranometer measurements are improved by adding temperature measurements using thermistors attached to the dome and detector of the pyranometer. The improved reflected solar TOA irradiances will be matched with CERES TOA SW fluxes derived from radiance measurements using angular modeling. Spatial discrepancy between the pyranometer footprint (75% of the energy in a 70km footprint) and the CERES footprint (20-80km depending on viewing zenith angle) must be accounted for in the comparison. Each balloon flight will provide at least 100 independent matching opportunities with each CERES instrument in orbit. The rotating scan plane capability of the CERES instrument could also be used to provide multiple observations (varying viewing geometry) each time the satellite flies directly above the ULDB. Such maneuvers require very accurate ULDB trajectory predictions. This is a new opportunity, with very modest cost to CERES, to compare TOA irradiances obtained from two independent missions. The engineering flight is scheduled for launch in January 2001. The first science mission is scheduled for December 2001. Additional information about the project and updated schedule are available at http://www.wff.nasa.gov/~uldb/.

5.4.2 Needs for Other Satellite Data

5.4.2.1 Aerosol Assimilations using Satellites

The earlier description of Class 2 Regional Climate Trend validation sites called attention to the use of ground-based aerosol monitoring to buttress the retrieval of surface albedo with satellite data. CERES has begun research from a related direction, namely the use of systematic aerosol assimilation products as a systematic “screen” for turbid skies. An aerosol assimilation (i.e.,

Collins et al., 2000, Rasch et al., 2000) is analogous to an NWP assimilation. The aerosol assimilation assumes climatological emissions of pollutants from industrial areas; includes a parameterization of wind blown dust as an source of aerosol; assimilates satellite retreivals of spectal AOT (Stowe et al., 1997; transports, nucleates, scavenges, and removes aerosols; is driven using a NWP re-analysis (here from NCEP). An aerosol product is then available under all sky conditions.

In CERES TRMM processing, there is no operational source of AOT over land. Hence, we have experimented with the Collins-Rasch assimilation, to date with a one month record. Over land, the assimilated AOT has been used with the Fu-Liou code and the SARB constrainment algorithm to retrieve surface albedo under clear conditions. Thru EOS Validation funding, we will obtain assimilated total AOT and species AOT at 630 nm; and vertical profiles of aerosol mixing ratios at 28 sigma levels. This will be tested for the TRMM domain of January-August 1998. While our initial target is an improved retrieval of surface albedo (i..e., comparison with the CARE campaign of August 1998 at SGP), the aerosol assimilation should be useful for estimating the vertical profile of aerosols and impacts on the heating rate. We have already compared a month of the Collins-Rasch assimilation with AERONET over 25 sites. The test of the 1998 assimilation will compare with existing records of the vertical profiles of extinction from the Raman lidar and backscatter from the MPL, both at SGP.

While direct validation of an aerosol assimilation under cloudy conditions would be difficult, the computed SARB surface and TOA fluxes that use the assimilation could be compared with measured fluxes, thereby validating the assimilation indirectly. The SARB calculations on Terra will use retrievals of aerosols from MODIS and possibly MISR. We will compare the Collins-Rasch assimilation for 1998, which uses AVHRR for aerosols, with the CERES TRMM VIRS aerosol retrievals. The 1998 experiment will be a preliminary run for the joint insertion of aerosol assimilated (Collins-Rasch, if then available) and directly retrieved (MODIS and MISR) aerosols in CERES Terra.

5.4.3 Measurement Needs

The measurement technology in greatest need of scientific advance is that for ground-based broadband solar insolation, as described in Section 5.2.2.4. The current technology is dated. Regarding deployment, the most needed measurement enhancements are the Class 2 Regional Climate Trend stations described in Section 5.2.2.

5.5 Implementation of Validation Results in Data Production

5.5.1 Special CERES Validation Data Products

The role of the on-line CAVE products in the validation of the SARB component of CERES has been

described earlier. Some CAVE products, such as the Long and Ackerman (2000) surface-based cloud screening, should be useful to other groups in EOS.

CERES uses 351 validation regions for special "subset" processing. Each region consists of all the CERES footprints that fall within a selected 1 by 1 degree gridbox. In subset processing, the CRS (SARB) software can be run over only these select regions; orders of magnitude faster than comprehensive global processing. This allows for quick testing of SARB algorithms and data sources. While most of the 351 regions have no ground observations, each CAVE validation site in Table 9 is generously covered by a set of validation gridboxes; the nearest four gridboxes (for a total of 2 by 2 degrees about each ground site) are included. This special validation subset processing has been run on an experimental basis to cover March and April 1998 for TRMM. An earlier form of the CERES Cloud WG (Minnis et al., 1997) retrievals were used. The following results (Figures 13-15) should NOT be taken as a representative of the final product from the SARB algorithm. The SURFACE observations used for comparison, however, should be regarded as near archival quality; the surface observations were take from ARM and EOS Validation Investigators Augustine, Dutton, Myers, and Pinker; they are available on CAVE. The TOA observations are an experimental SSF product; they are not yet archived, but should be of higher quality than the archived "ERBE-like" ES8 CERES TOA fluxes available on CAVE.

Figure 13 (see next page) shows the scatterplots for clear conditions, as identified by the CERES cloud mask (VIRS imager on TRMM), for surface fluxes: LW down, SW down, LW up, and SW up. For each point, we have matched the CERES footprint (much smaller than a 1 by 1 degree gridbox) observation with the untuned (uncontrained) flux computed by Fu-Liou. ECMWF temperature and humidity profiles, originally 0.56 by 0.56 degree on a 6-hourly basis, were here interpolated to the 1 by 1 gridbox and single hour nearest the instantaneous footprint. The surface LW in the shows a good match of "Model" (computed) with "Obs" (observation). Over the large geographical range of CAVE (Table 9), the observed DLF is 2.6 Wm-2 larger than computed (upper left of Figure 13); this is similar to Figure 8 for the clear-sky CAGEX Version 2.2.0, which had the benefit of collocated 3-hourly radiosonde data at SGP. The computation of upward LW surface flux (lower left in Figure 13) benefits from a CERES clear-sky VIRS retrieval of skin temperature.

Figure 13 see next page **Comparison of SARB Fu-Liou Model (untuned) with CAVE surface sites of Table 9. Clear skies identified by VIRS satellite imager. ECMWF profiles and VIRS skin temperature. Day only. TRMM February-March 1998.**

Clear Sky (SSF Cld Frac = 0.0) Daytime Surface Fluxes
CERES/SARB Calculations Matched to CAVE Surface Observations

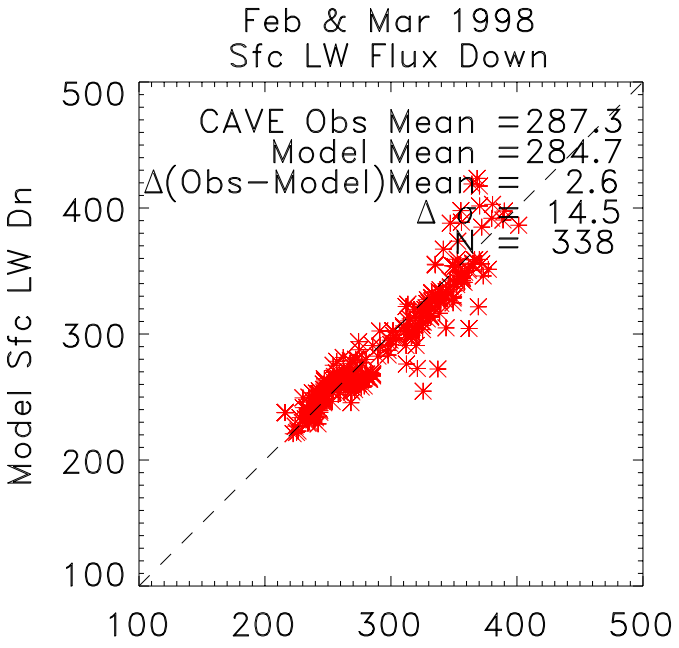

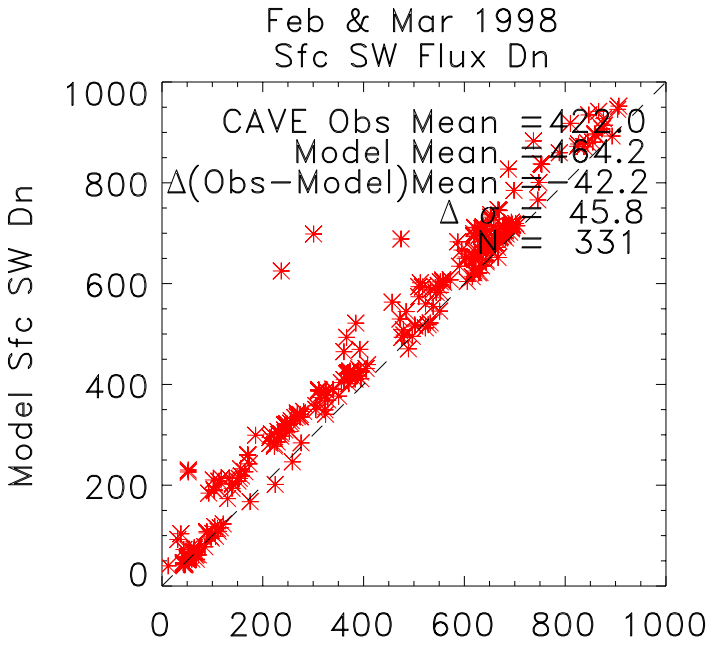

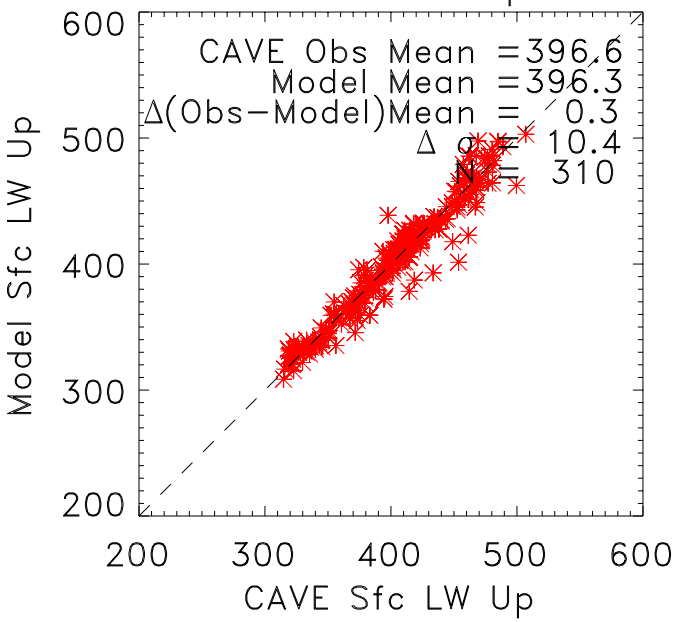

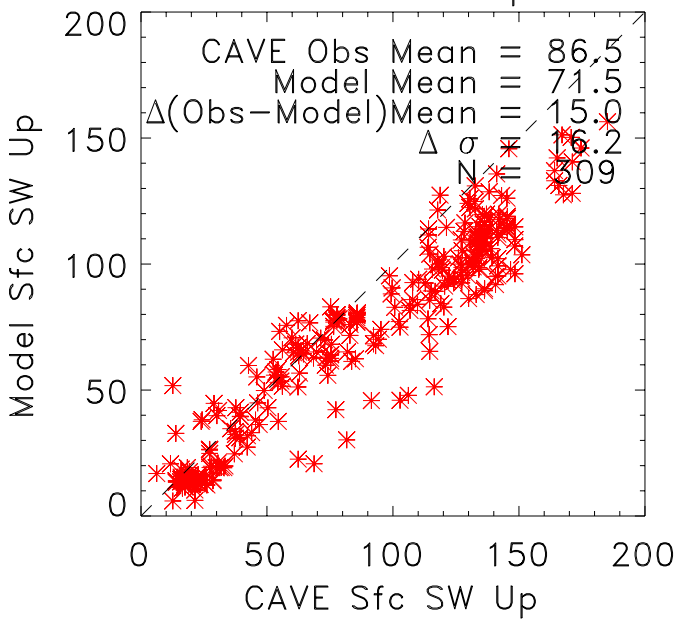

The computed SW insolation (upper right in Figure 13) exceeds the observation by 42.2 Wm-2. This large discrepancy is comparable to those found in CAGEX Version 1 and Kato et al. (1997). Here it is likely due to the application of monthly mean AOT from the GFDL Chemical Transport Model (CTM). This is a production test, so we have not used any available AOT from sunphotometers on CAVE. We will attempt to better this production using the 6-hourly Collins-Rasch aerosol assimilation.

In Figure 14 (see next page) we restrict the domain to those footprints which are screened as clear by the Long and Ackerman (2000) surface-based, high-frequency time series method. The screening was here not available for about half of the CAVE sites. But the screen is tight, restricting the domain further by a factor of ten. Cases of reflection from cloud side walls have apparently been removed. In satellite-only cloud screening the standard deviation for insolation was 45.8 Wm-2 (right top of Figure 13), as opposed to the stringent Long-Ackerman screening that reduces the standard deviation to 24.0 Wm-2 (right top of Figure 14). The mean differences in Figures 13 are close to the respective differences in Figure 14; this suggests that the mean CERES VIRS cloud mask compares well with the Long-Ackerman surface technique. The clear-sky results shown here were restricted to daytime only, as Long-Ackerman requires SW measurements.

The all-sky (total sky) comparison is shown in Figure 15 (see next page). The approximate magnitude as “model minus observation” differs little for clear sky versus total sky in LW and SW, upwelling and downwelling. The upper left panel of Figure 15 shows a small group of extreme outliers; model LW down greatly exceeding observations; these are likely clear scenes for the radiometer at a point, wherein the satellite identified low clouds somewhere in the footprint (and probably at night).

This method will be extended to other components of CERES processing. Here, we have compared instantaneous satellite retreivals with half-hourly mean surface observations. In CERES Time and Space Averaging (TISA), 3-hourly and daily mean fluxes will be computed and compared with CAVE observations. Figures 13-15 compare radiative fluxes. We will also compare with input parameters, such as AOT.

Figure 14 (see next page) **As Figure 13, but clear skies further screened using surface radiometer time series and domain is now only a subset of Table 9.**

Figure 15 (see next page) **As Figure 13, but for total-sky (all-sky, full-sky) and day plus night. Cloud height, optical depth, and fractional area from VIRS (Minnis et al., 1997, CERES Subsystem 4). No tuning (constrainment).**

Clear Sky (Surface Radiometry Cld Frac = 0.0) Daytime Surface Fluxes
CERES/SARB Calculations Matched to CAVE Surface Observations

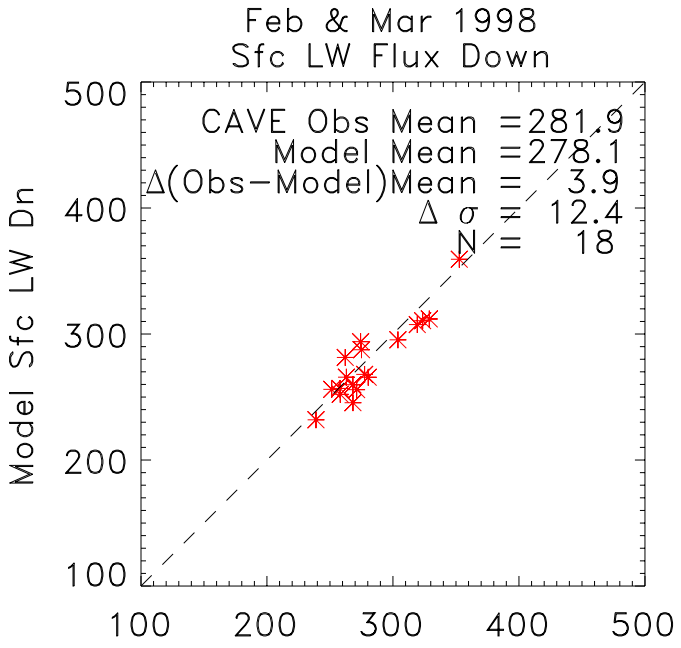

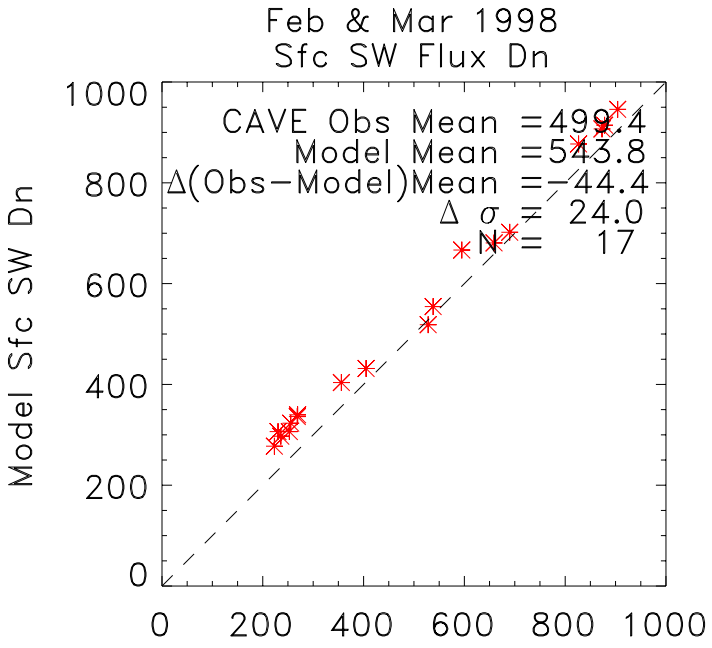

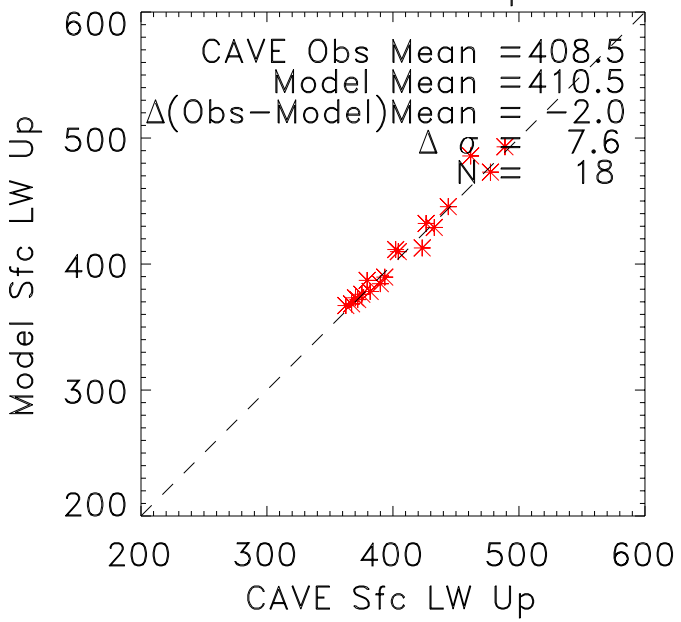

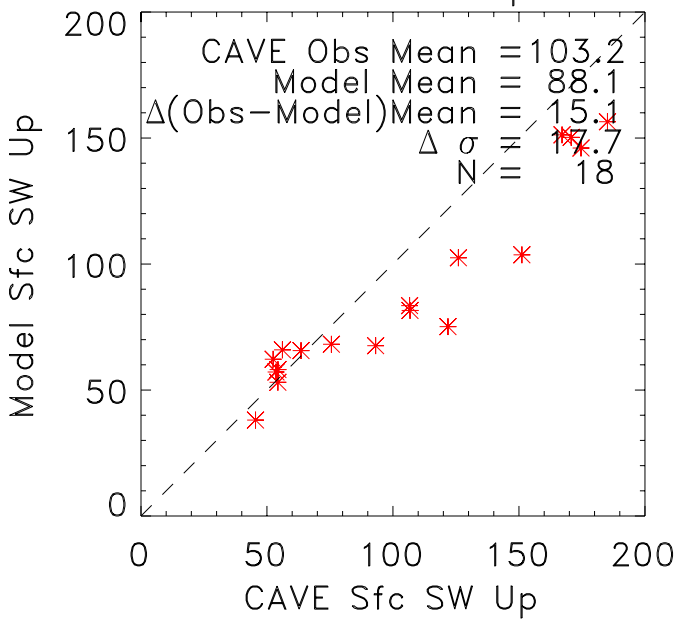

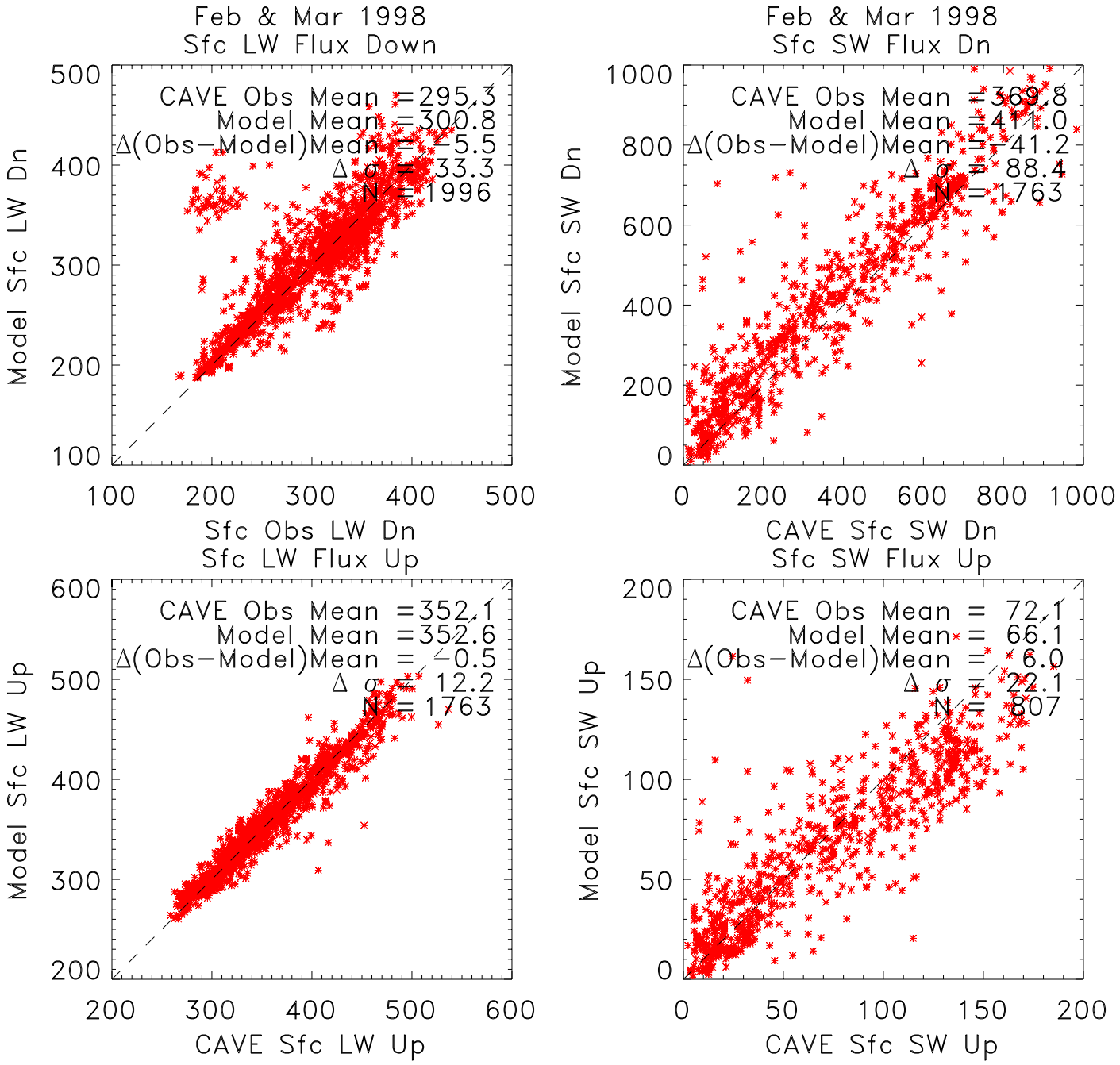
All Sky Surface Flux(W/m²), Day & Night
CERES/SARB Calculations Matched to CAVE Surface Observations
Feb & Mar 1998
Sfc LW Flux Down
CAVE Obs Mean =295.3
Model Mean =300.8
Δ(Obs−Model)Mean = −5.5
Δ σ = 33.3
N = 1996
Model Sfc LW Dn
Sfc Obs LW Dn
Feb & Mar 1998
Sfc SW Flux Dn
CAVE Obs Mean =369.8
Model Mean =411.0
Δ(Obs−Model)Mean = −41.2
Δ σ = 88.4
N = 1763
Model Sfc SW Dn
CAVE Sfc SW Dn
Sfc LW Flux Up
CAVE Obs Mean =352.1
Model Mean =352.6
Δ(Obs−Model)Mean = −0.5
Δ σ = 12.2
N = 1763
Model Sfc LW Up
CAVE Sfc LW Up
Sfc SW Flux Up
CAVE Obs Mean = 72.1
Model Mean = 66.1
Δ(Obs−Model)Mean = 6.0
Δ σ = 22.1
N = 807
Model Sfc SW Up
CAVE Sfc SW Up

5.5.2 Validation Procedures and Milestones

Procedures are described in Section 5.5.1 (Special CERES Validation Data Products). The principal milestone will be the automation of this process for a larger number of tunable variables (i.e., the adjustments to cloud properties, AOT, PW, and skin temperture) and the constrained fluxes. This document only compares untuned fluxes (i.e., Figures 13-15). Archival for this component of CERES is still at least one year away, even for the earlier TRMM data which starts in December 1997.

Ad hoc investigation of tunable parameters has been fruitful. In our constrainment algorithm, the main tuning parameters over clear ocean are skin temperature, lower troposheric humidity (LTH), upper tropospheric humidity (UTH), skin temperature, and AOT. Over the tropical ocean, we have found that the Wentz TMI skin temperatures and precipitable water (PW) are better inputs for the computation of clear sky LW paratmeters than are the ECMWF variables in current use. For example, consider a comparison of simulated and observed radiation at over 200,000 clear sky ocean footprints for March 7-9, 2000. Figure 16 (see next page) shows differences (Fu-Liou simulated minus CERES observed) for LW filtered window and LW broadband unfiltered radiances. These are plotted versus the differences of (1) the "MOA" inputs used by CERES in the Fu-Liou calculation minus (2) values of the same quantities retrieved by TRMM Tropical Microwave Imager (TMI). CERES "MOA" SST and PW are from ECMWF; ECMWF SST is essentially the NOAA Reynolds AVHRR blended analysis. The TMI products were pulled from the Remote Sensing Systems (RSS) URL (www.ssmi.com), i.e. Wentz et al. (2000). The differences of computed and observed filtered window (left panels of Figure 16) are only 0.1 Wm-2sr-1. But the upper left panel shows that if the MOA SST (used for the computation) were replaced by the TMI SST, the untuned filter window computation would be reduced when higher than observations (and increased when lower than observations). The differences of computed and observed LW radiances for the unfiltered broadband are larger than for the filtered window; the mean difference for broadband radiance has a magnitude in excess of –1 Wm-2sr-1 (about –3 Wm-2 in flux). The lower right panel of Figure 16 shows that the errors in computed broadband are due mostly to values of PW in MOA (ECMWF) that are too high; if we used the PW from TMI, the computed broadband would be systematically closer to the observations. Additional analysis (not shown) suggests the the impact on broadband is mostly thru a correlation of PW and UTH.

Figure 16 (see next page) **Differences of CERES LW radiances (computed minus observed) versus input values (CERES MOA minus TMI) used in radiative transfer calculation. Clear-sky tropical ocean March 7-9, 2000.**

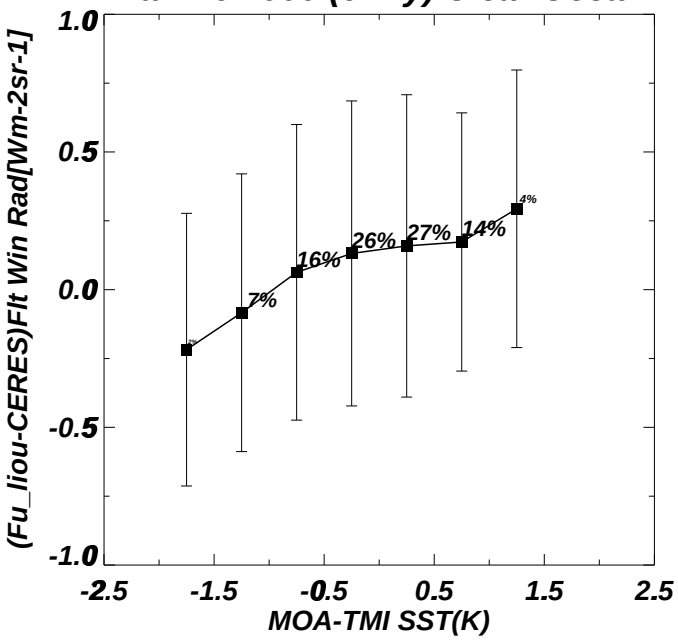

N= 225883
Mean (Std.Dev)
MOA-TMI SST(K) : -0.09 (0.73)
(Fu_liou-CERES)Flt Win Rad[Wm-2sr-1] : 0.12 (0.54)

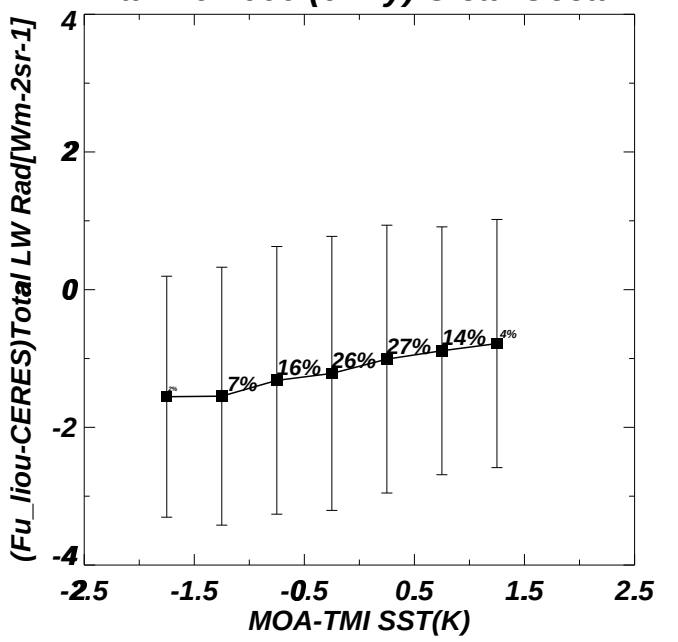

N= 225883
Mean (Std.Dev)
MOA-TMI SST(K) : -0.09 (0.73)
(Fu_liou-CERES)Total LW Rad[Wm-2sr-1] : -1.13 (1.93)

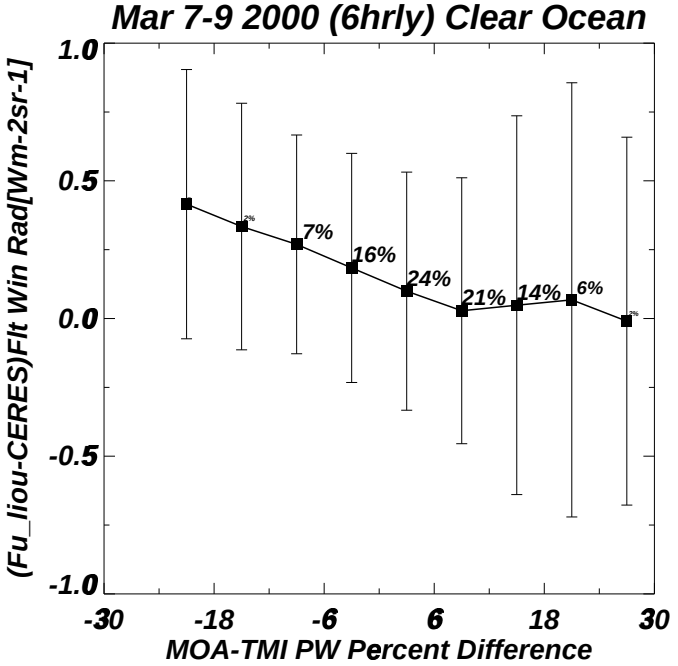

N= 251540
Mean (Std.Dev)
MOA-TMI PW Percent Difference : 5.59 (10.83)
(Fu_liou-CERES)Flt Win Rad[Wm-2sr-1] : 0.11 (0.53)

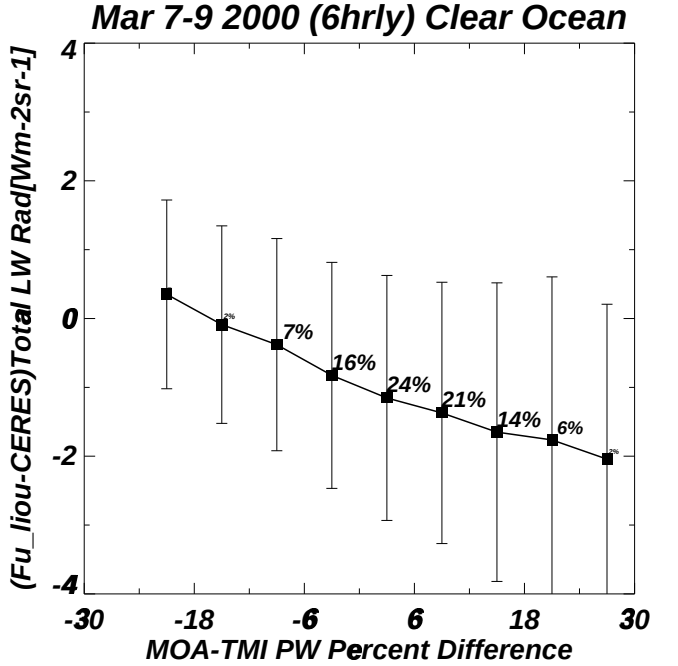

N= 251540
Mean (Std.Dev)
MOA-TMI PW Percent Difference : 5.59 (10.83)
(Fu_liou-CERES)Total LW Rad[Wm-2sr-1] : -1.18 (1.95)

5.5.3 Role of EOSDIS

No conspicuous role.

5.6 Summary

Our goal in this component of CERES is to extend the spatial and temporal domain over which the Surface and Atmospheric Radiation Budget (SARB; the vertical profile of radiative fluxes) can be specified with useable accuracy.

The place of the SARB in CERES processing is summarized in the earlier Table 1. The concepts for validation are in the earlier Table 2. The main validation activities are described in the earlier Table 3.

Validation of this component of CERES began well before launch with the CERES/ARM/GEWEX Experiment (CAGEX). CAGEX Versions 1 and 2 (Charlock and Alberta, 1996) provide on-line access to the input data for the pre-launch SARB retrievals, the retrieved fluxes, and validating measurements over the ARM CART SGP site (http://snowdog.larc.nasa.gov:8081/cagex.html).

For post-launch validation, the on-line CERES ARM Validation Experiment CAVE provides observations of ground-based radiation data over a few score ARM, BSRN, SURFRAD, CMDL, and other sites worldwide. CAVE emphasizes the use of calibrated and collocated of sets of instruments to enhance closure with continuous and long-term measurements; CAVE provides ready access to these and to collocated, conveniently subset CERES TOA data. See earlier Figure 1 and http://www-cave.larc.nasa.gov/cave/ for CAVE overview; Figure 11 and Table 9 for CAVE sites.

Because of the unique power of over-water measurements for the validation of the upwelling surface radiation retrieved by satellites, CERES has begun its own measurement program at an ocean site. The CERES Ocean Validation Experiment (COVE) at the Chesapeake Lighthouse is regarded as useful by MODIS-Atmospheres, MISR, and GACP, which have joined forces with CERES for the Chesapeake Lighthouse and Aircraft Measurements for Satellites (CLAMS) field campaign in summer 2001. A low level OV-10 aircraft, the CERES Fixed-wing Airborne Radiometer (C-FAR), will be used in CLAMS with an ER-2 and CV-580. C-FAR will be a useful tool for the validation of CERES and other components of EOS over land surfaces. See earlier Figure 6 for COVE overview; find field campaign information by clicking “CLAMS” at http://www-cave.larc.nasa.gov/cave/; see earlier Figure 12 on C-FAR and OV-10.

Continuing with the CAVE theme, a Class 2 "Regional Climate Trend" set of validation sites is suggested for EOS-wide application (see Section 5.2.1). Class 2 sites are based on existing or planned networks outside of EOS, but supplementary EOS measurements are needed. Many are on-line at CAVE. Class 2 sites observe broadband surface radiation, spectral AOT, and surface meteorology; this suite of observations enables a researcher to validate the

"subtraction of the atmosphere" by EOS. By combining MISR, MODIS, ASTER, and CERES TOA measurements and SARB calculations with Class 2 data, we will be able to accurately distinguish and monitor trends in the elusive climate forcings of anthropogenic aerosols (Penner et al., 1994) and land use changes. Current climate forcing assessments (see IPCC 1995 and subsequent documents in series) are very weak on aerosols and surface albedo. The Class 2 sites will be able to monitor the impact of the direct effect of aerosols (scattering and absorption), but not necessarily the indirect effect of aerosols; it may be possible to infer CCN effects as a residual.

An improvement in measurement technology for broadband in situ flux is definitely needed. CERES has here assisted the community by testing new methods, such as the fitting of thermistors to the domes of pyranometers (Figure 17 see next page) by Haeffelin et al., 2000. The new methods will be exploited for SARB validation by measuring upwelling fluxes in situ at 35 km during Ultra-Long Duration Balloon (ULDB) flights; these have long duration (~90 days) and are highly cost effective for CERES.

Related measurements needed for validation include the single scattering albedo of aerosols (i.e., Heintzenberg, et al., Mlawer et al., 2000) and clouds, and the ground-based remote sensing of cloud properties. These are available at a handfull of sites. It is presently difficult to evaluate their quality. Comparison of theory and observation proved to be important in the evaluation of the broadband in situ measurements. CERES SARB validation has been useful in evaluating NWP analyses (i.e., Figure 16), and validation over the principal ARM sites may be useful in evaluating new instruments and new remote sensing products (i.e., Dubovik and King, 2000), too. Modifications to the Langley Fu-Liou code are underway to incorporate cloud inhomogeneity (Kato and Smith, 2000) and other factors in tests prior to archival.

Figure 17 (see next page) **Modification to improve pyranometer used in validation of CERES retrievals for SW insolation at surfaceG**

Improving Measurements for CERES Validation: Diffuse Solar Irradiances Measured by Standard and Modified Eppley PSP

Modified PSP uses body and dome temperature measurements to remove the spurious infrared contribution to the signal

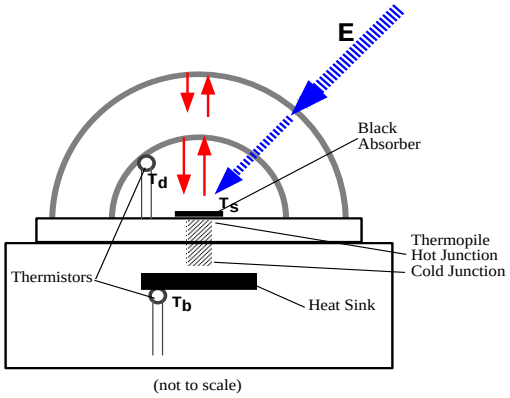

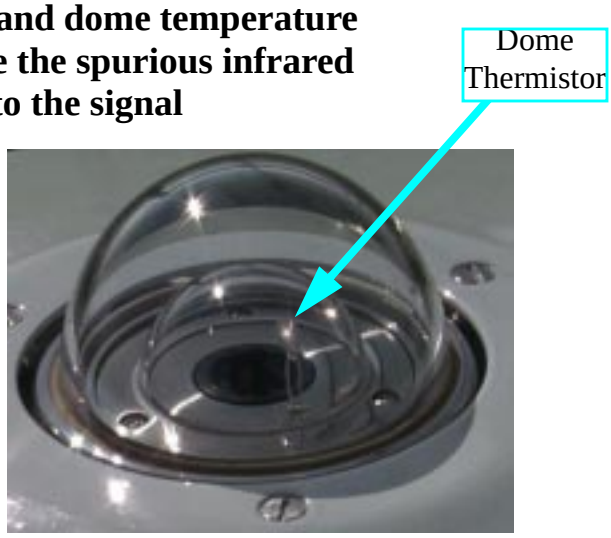

Diurnal Cycle of Diffuse Solar Irradiance at NASA LaRC

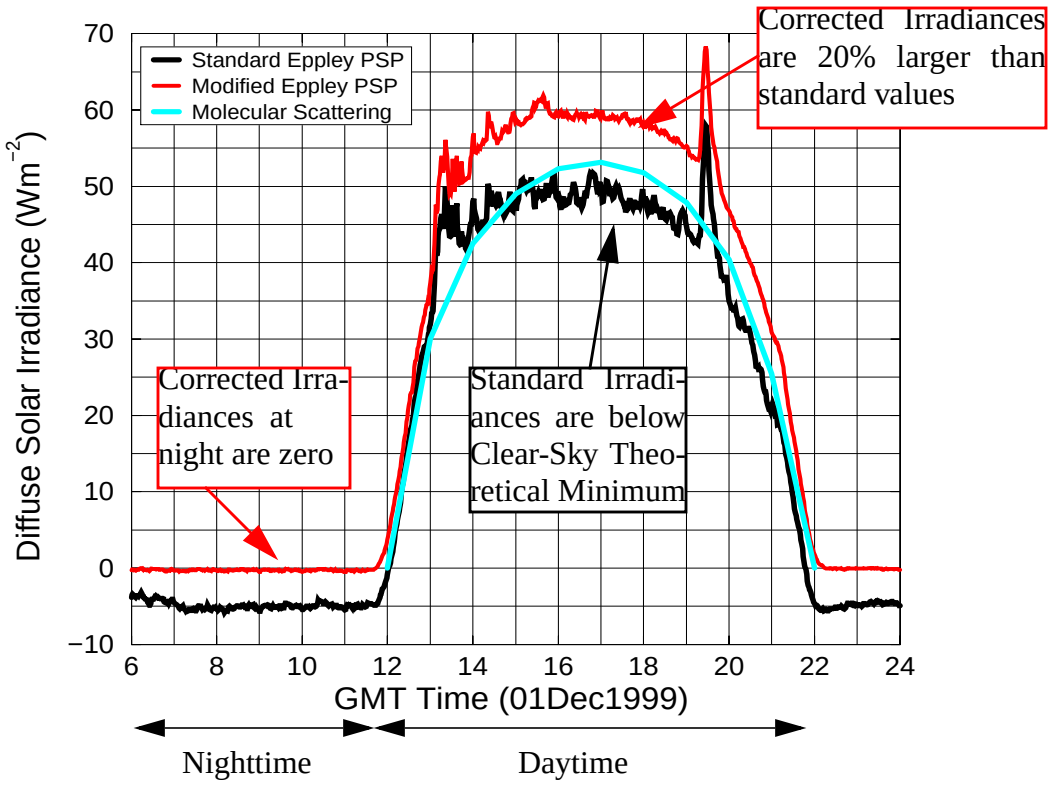

Martial Haeffelin - Virginia Tech/NASA LaRC - 04/05/2000

5.7 References

Alberta, T. L., and T. P. Charlock, 1999: A comprehensive resource for the investigation of shortwave fluxes in clear conditions: CAGEX Version 3. Proceedings of the AMS Tenth Conference on Atmospheric Radiation, Madison WI (June 28 – July 2, 1999), 279-282.

Alberta, T. L., T. P. Charlock, C. H. Whitlock, F. G. Rose, R. DiPasquale, R. Pinker, W. F. Staylor, and S. Gupta, 1994: Climate observations with GEWEX Surface Radiation Budget Project data. Proceedings of the AMS Eighth Conference on Atmospheric Radiation, Nashville TN (January 23-28, 1994), 22-24 pp.

Anderson, G. P., et al., 1995: MODTRAN3: Suitability as a flux-divergence code. In Proceedings of the 4th ARM Science Team Meeting (1994), DOE Rep. CONF-940277, U.S. Dep. of Energy, Washington, D.C., pp. 75-80.

Asano, S., A. Uchiyama, Y. Mano, M. Murakami, and Y. Takayama, 2000: No evidence for solar absorption anomaly by marine water clouds through collocated aircraft radiation meaurements. J. Geophys. Res., 105, 14,761-14,775.

Augustine, J. A., J. J. DeLuisi, and C. N. Long, 2000: SURFRAD – A national surface radiation budget network for atmospheric research. Bull. Amer. Meteor. Soc., in press.

Barkstrom, B., E. Harrison, G. L. Smith, R. Green, J. Kibler, R. Cess, and the ERBE Science, 1989: Earth Radiation Budget Experiment (ERBE) archival and April 1985 results. Bull. Amer. Meteor. Soc., 70, 1254-1262.

Barnett, T. P., J. Ritchie, J. Foat, and G. Stokes, 1998: On the space-time scales of the surface solar radiation field. J. Clim., 11, 88-96.

Briegleb, B. P., P. Minnis, V. Ramanathan, and E. Harrison, 1986: Comparison of regional clear-sky albedos inferred from satellite observations and model computations. J. Climate Appl. Meteor., 25, 214-226.

Bush, B. C., F. P. J. Valero, A. Sabrina Simpson, and L. Bignone, 2000: Characterization of thermal effects in pyranometers: A data correction algorithm for improved measurement of surface insolation. J. of Atmos. Ocean. Tech., 17, 165-175.

Cess, R. D., M. H. Zhang, P. Minnis, L. Corsetti, E. G. Dutton, B. W. Forgan, D. P. Garber, W. L. Gates, J. J.

Hack, E. F. Harrison, X. Jing, J. T. Kiehl, C. N. Long, J.-J. Morcrette, G. L. Potter, V. Ramanathan, B. Subasilar, C. H. Whitlock, D. F. Young, and Y. Zhou, 1995: Absorption of solar radiation by clouds: Observations versus models. Science, 267, 496-499.

Charlock, T., and T. Alberta, 1996: The CERES/ARM/GEWEX Experiment (CERES) for the retrieval of radiative fluxes with satellite data. Bull. Amer. Meteor. Soc., 77, 2673-2683.

Charlock, T., F. Rose, T. Alberta, G. L. Smith, D. Rutan, N. Manalo-Smith, T. D. Bess, and P. Minnis, 1994: Retrievals of the Surface and Atmospheric Radiation Budget: Constrainment Parameters with Radiative Transfer to Balance Pixel-Scale ERBE Data. Eighth Conference on Atmospheric Radiation. American Meteorological Society. Nashville, Tennessee, January 23-28, 1993, 435-437.

Charlock, T., F. Rose, T. Alberta, G. L. Smith, D. Rutan, N. Manalo-Smith, P. Minnis, and B. Wielicki, 1994: Cloud profiling radar requirements: Perspective from the retrievals of the surface and atmospheric radiation budget and studies of atmospheric energetics. Report of GEWEX Topical Workshop on Utility and Feasibility of a Cloud Profiling Radar. WMO/TD No. 593, B10-B-29.

Charlock, T. P., F. G. Rose, T. L. Alberta, and G. D. Considine, 1998: Comparison of computed and measured cloudy-sky shortwave (SW) in the ARM Enhanced Shortwave Experiment (ARESE). Proceedings of ARM Science Team Meeting, Tuscon, AZ, March 23-27, 1998 (available at the URL www.arm.gov).

Charlock, T. P., F. G. Rose, and T. L. Alberta, 1999: An observational study of cloud forcing to the atmospheric absorption of SW over Kansas and Oklahoma for January-August 1998. Proceedings of the AMS Tenth Conference on Atmospheric Radiation, Madison WI (June 28 – July 2, 1999), 262-265.

Charlock, T., F. Rose, D. Rutan, L. Coleman, B. Baum, and R. Green, 1997: The total-sky, global atmospheric radiation budget from radiative transfer calculations using ERBE, AVHRR, and sounding data. Proceeding of the Ninth Conference on Atmospheric Radiation, Long Beach (Feb. 2-7, 1997), AMS, 60-63. [See more extensive document on http://asd-www.larc.nasa.gov/ceres/trmm/atdbs.html by clicking “Subsystem 5.0”]

Charlock, T. P., F. G. Rose, D. A. Rutan, T. L. Alberta, D. P. Kratz, L.H. Coleman, G. L. Smith, N. Manalo-Smith, and T. D. Bess, 1997: Compute Surface and Atmospheric Fluxes

(System 5.0), CERES Algorithm Theoretical Basis Document. 84 pp. See http://asd-www.larc.nasa.gov/ATBD/.

Chou, M.-D., A. Arking, J. Otterman, and W. L. Ridgway, 1995: The effect of clouds on atmospheric absorption of solar radiation. Geophys. Res. Lett., 22, 1885-1888.

Chou, M.-D., and M. J. Suarez, 1999: A solar radiation parameterization for atmospheric studies. NASA/TM-1999-104606, Vol. 15, 40 pp.

Collins, W. D., and A. K. Inamdar, 1995: Validation of clear-sky fluxes for tropical oceans from the Earth Radiation Budget Experiment. J. Climate, 8, 569-578.

Collins, W. D., P. J. Rasch, B. E. Eaton, B. V. Khattatov, J.-F. Lamarque, and C. S. Zender, 2000: Simulating aerosols using a chemical transport model with assilimiation of satellite aerosol retrievals: Methodology for INDOEX. Accepted by J. Geophys. Res..

Cox, C. S., and W. Munk, 1954: Statistics of the sea surface derived from sun glitter. J. Mar. Res. 13, 198-225.

Cox, C. S., and W. Munk, 1955: Some problems in optical oceanography. J. Mar. Res. 14, 63-78.

d'Almeida, G., P. Koepke, and E. P. Shettle, 1991: Atmospheric Aerosols - Global Climatology and Radiative Characteristics. A. Deepak Publishing, Hampton, Virginia. 561 pp.

Darnell, W. L., W. F. Staylor, S. K. Gupta, N. A. Ritchey, and A. C. Wilber, 1992: Seasonal variation of surface radiation budget derived from International Satellite Cloud Climatology Project C1 data. J. Geophys. Res., 97, 15741-15760.

DeLuisi, J., 1991: Second Workshop on Implementation of the Baseline Surface Radiation Network. WCRP-64, WMO/TD No. 453.

Dubovik, O., and M. D. King, 2000: A flexible inversion algorithm for retrieval of aerosol optical properties from Sun and sky radiance measurements. J. Geophys. Res., 105, 20,673-20,696.

Dutton, E. G., J. J. Michalsky, T. Stoffel, B. W. Forgan, J. Hickey, D. W. Nelson, T. L. Alberta, and I. Reda, 2000: Measurement of broadband diffuse solar irradiance using current commercial instrumentation with a correction for thermal offset errors. Accepted by J. Atmos. Ocean. Tech.

Ellingson, R. G., J. Ellis, and S. Fels, 1991: The intercomparison of radiation codes in climate models (ICRCCM): Longwave results. J. Geophys. Res., 96, 8929-8953.

Ellingson, R. G., and Y. Fouquart, 1990: Radiation and climate: Intercomparison of Radiation Codes in Climate Models (ICRCCM). World Climate Research Program-39, 38 pp.

Ellingson, R. G., D. Yanuk, A. Gruber, and A. J. Miller, 1994: Development and application of remote sensing of longwave cooling from the NOAA polar orbiting satellites. Photogrammetric Engineering and Remote Sensing, 60, 307-316.

Ellingson, R. G., and W. J. Wiscombe, 1995: The Spectral Radiance Experiment (SPECTRE): Project description and sample results. Submitted to Bull. Amer. Meteor. Soc.

Feltz, W. F., W. L. Smith, R. O. Knuteson, H. E. Revercomb, H. M Woolf, and H. B. Howell, 1998: Meteorological applications of temperature and water vapor retrievals from the ground-based Atmospheric Emitted Radiance Interferometer (AERI). J. Appl. Meteor., 37, 857-875.

Fu, Q., B. Carlin, and G. Mace, 2000: Cirrus horizontal homogeneity and OLR bias. Submitted to Geophys. Res. Lett.

Fu, Q., G. Lesins, J. Higgins, T. Charlock, P. Chylek, and J. Michalsky, 1998: Broadband water vapor absorption of solar radiation tested using ARM data. Geophys. Res. Lett., 25, 1169-1172.

Fu, Q., and K.-N. Liou, 1993: Parameterization of the radiative properties of cirrus clouds. J. Atmos. Sci., 50, 2008-2025.

Fu, Q., K. Liou, M. Cribb, T. Charlock, and A Grossman, 1997: On multiple scattering in thermal infrared radiative transfer. J. Atmos.

Fu, Q., W.B. Sun, and P. Yang, 1999: Modeling of scattering and absorption by nonspherical cirrus ice particles at thermal infrared wavelengths. J. Atmos. Sci., 56, 2937-2947.

Gilgen, H., C. H. Whitlock, F. Koch, G. Mueller, A. Ohmura, D. Steiger, and R. Wheeler, 1995: Technical Plan for Baseline Surface Radiation Network (BSRN) Data Manangement. World Climate Research Program. WMO TD-No. 443.

Gupta, S., 1989: A parameterization for longwave surface radiation f sun-synchronous satellite data. J. Climate, 2, 305-320.

Gupta, S. K., W. L. Darnell, and A. C. Wilber, 1992: A parameterization for longwave surface radiation from satellite data: Recent improvements. J. Appl. Meteor., 12, 1361-1367.

Haeffelin, M., S. Kato, A. M. Smith, K. Rutledge, T. Charlock, and J. R. Mahan, 2000: Determination of the thermal offset of the Eppley Precision Spectral Pyranometer. Submitted to Appl. Opt.

Halthore, R. N., S. Nemesure, S. E. Schwartz, D. G. Imre, A. Berk, E. G. Dutton, and M. H. Bergin, 1998: Models overestimate diffuse clear-sky surface irradiance: A case for excess atmospheric absorption. Geophys. Res. Lett., 25, 3591-3594.

Harrison, E. F., P. Minnis, B. R. Barkstrom, V. Ramanathan, R. D. Cess, and G. G. Gibson, 1990: Seasonal variation of cloud radiative forcing derived from the Earth Radiation Budget Experiment. J. Geophys. Res., 95, 18687-18703.

Harrison, L., J. Michalsky, and J. Berndt, 1994: Automated multifilter rotating shadow-band radiometer: An instrument for optical depth and radiation measurements. Appl. Opt., 33, 5118-5132.

Hayasaka, T., N. Kikuchi, and M. Tanaka, 1995: Absorption of solar radiation by stratocumulus clouds: Aircraft measurements and theoretical calculations. J. Appl. Meteor., 34, 1047-1055.

Heintzenberg, J., R. J. Charlson, A. D. Clarke, C. Liousse, V. Ramaswamy, K. P. Shine, M. Wendisch, and G. Helas, 1997: Measurements and modelling of aerosol single scattering albedo: Progress, problems, and prospects. Beitr. Phys. Atmosph., 70, 249-263.

Hess, M., P. Koepke, and I. Schult, 1998: Optical Properties of Aerosols and Clouds: The software package OPAC. Bull. Amer. Meteor. Soc., 79, 831-844.

Hicks, B. B., J. J. DeLuisi, and D. R. Matt, 1995: The NOAA Integrated Surface Irradiance Study (ISIS) - a new surface radiation monitoring program. Submitted to Bull. Amer. Meteor. Soc.

Holben, B. N., T. F. Eck, I. Slutsker, D. Tanre, J. P. Buis, A. Setzer, E. Vermote, J. A. Reagan, Y. J. Kaufman, T. Nakajima, F. Lavenu, I. Jankowiak, and A. Smirnov, 1998: AERONET – A federated instrument network and data archive for aerosol characterization. Remote Sens. Environ., 66, 1-16.

Intergovernmental Panel on Climate Change (IPCC), 1995: Climate Change 1995. The Science of Climate Change. Houghton, J. T., et al., Eds., Cambridge University Press. 572 pp.

Kato, S., T. P. Ackerman, E. E. Clothiaux, J. H. Mather, G. R. Mace, M. Wesley, F. Murcray, and J. Michalsky, 1997: Uncertainties in modeled and measured clear-sky surface shortwave irradiances. J. Geophys. Res., 102, 25,881-25,898.

Kato, S., T. P. Ackerman, E. G. Dutton, N. Laulainen, and N. Larson, 1999a: A comparison of modeled and measured surface shortwave irradiance for a molecular atmosphere, J. Quant. Spectrosc. Radiat. Transfer., 61, 493-502.

Kato, S., M. H. Bergin, T. P. Ackerman, T. P. Charlock, E. E. Clothiaux, R. A. Ferrare, R. N. Halthore, N. Laulainen, G. G. Mace, J. Michalsky, and D. D. Turner, 1999b: A comparison of the aerosol optical thickness derived from ground-based and airborne measurements. J. Geophys. Res., 105, 14,701-14,717.

Kato, S., and G. L. Smith, 2000: Computation of the domain averaged irradiance by the discrete ordinate radiative transfer algorithm. Submitted to J. Atmos. Sci.

Levitus, S., J. I. Antonov, T. P. Boyer, and C. Stevens, 2000: Warming of the world ocean. Science, 287, 2225-2228.

Li, Z., H. W. Barker, and L. Moreau, 1995: The variable effect of clouds on atmospheric absorption of solar radiation. Nature, 376, 486-490.

Li, Z., P. Wang, and J. Cihlar, 2000: A simple and efficient method for retrieving surface UV radiation dose rate from satellite. J. Geophys. Res., 105, 5027-5036.

Li, Z., and H. Leighton, 1993: Global climatologies of solar radiation budgets at the surface and in the atmosphere from 5 years of ERBE data. J. Geophys. Res., 98, 4919-4930.

Lin, B., S. J. Katzberg, J. L. Garrison, and B. A. Wielicki, 1999: Relationship between GPS signals reflected from sea surfaces and surface winds: Modeling results and comparisons with aircraft measurements. J. Geophys. Res., 104, 20,713-20,727.

Liou, K. N., 1992: Radiation and Cloud Processes in the Atmosphere. Oxford University Press, 487 pp.

Long, C. N., and T. P. Ackerman, 2000: Identification of clear skies from broadband pyranometer measurements and

calculation of downwelling shortwave cloud effects. J. Geophys. Res., 105, 15,609-15,626.

Lubin, D., E. H. Jensen, and H. P. Gies, 1998: Global surface ultraviolet radiation climatology from TOMS and ERBE data. J. Geophys. Res., 103, 26,061-26,092.

Mace, G. G., K. Sassen, S. Kinne, and T. P. Ackerman, 1998: An examination of cirrus cloud characteristics using data from millimeter wave radar and lidar. Geophys. Res. Lett., 25, 1133-1136.

Major, S., D. R. Doelling, M. M. Khaiyer, P. Minnis, and D. R. Cahoon, Jr., 1999: Surface bidirectional reflectance functions derived from CERES helicopter data or the ARM Southern Great Plains Site. Proceedins of the AMS Tenth Conference on Atmospheric Radiation. Madison WI (June 28 – July 2, 1999), 540-543.

Minnis, P., W. L. Smith, Jr., D. P. Garber, J. K. Ayers, and D. R. Doelling, 1995: Cloud properties derived from GOES-7 for spring 1994 ARM Intensive Observing Period using Version 1.0.0 of ARM satellite data analysis program. NASA Reference Publication 1366, 58 pp.

Minnis, P., D. F. Young, D. P. Kratz, J. A. Coakley, Jr., M. D. King, D. P. Garber, P. W. Heck, S. Major, and R. F. Arduini, 1997: Cloud optical property retrieval. (System 4.3), CERES Algorithm Theoretical Basis Document. 60 pp. See http://asd-www.larc.nasa.gov/ATBD/.

Mishchenko, M. I., and L. D. Travis, 1997: Satellite retrieval of aerosol properties over ocean using polarization as well as intensity of reflected sunlight. J. Geophys. Res., 103, 16989-17013.

Mlawer, E. J., P. D. Brown, S. A. Clough, L. C. Harrison, J. J. Michalsky, P. W. Kiedron, and T. Shippert, 2000: Comparison of spectral direct and diffuse solar irradiance measurments and calculations for cloud free conditions. Submitted to Geophys. Res. Lett.

Mlawer, E. J., S. J. Taubman, P. D. Brown, M. J. Iacono, and S. A. Clough, 1997: Radiative transfer for inhomogeneous atmospheres: RRTM, a validated correlated-k model for the longwave. J. Geophys. Res., 102, 16,663-16,682.

Myers, D. R., S. Wilcox, M. Anderberg, S. H. Alawaji, N. Al-Abbadi, and M. Y. bin Mahfoodh, 1999: Saudi Arabian Solar Radiation Network and Data for Validating Satellite Remote Sensing Systems. Earth Observing Systems IV, Vol. 3750 of the Society for Photo-Optical Instrumentation

Engineers (SPIE) Annual Conference in Denver, CO, July 18-22.

Payne, R. E., 1972: Albedo of the sea surface. J. Atmos. Sci. 29, 959-970.

Pilewskie, P., and F. P. J. Valero, 1995: Direct observations of excess solar absorption by clouds. Science, 267, 1626-1629.

Pinker, R., and I. Laszlo, 1992: Modeling surface solar irradiance for satellite applications on a global scale. J. Appl. Meteor., Vol. 31, 194-211.

Rabier, F., J.-N. Thepaut, and P. Courtier, 1998: Extended assimilation and forecast experiments with a four-dimensional variational assimilation. Quart. J. Roy. Meteor. Soc., 124, 1861-1887.

Ramanathan, V., B. Subasilar, G. J. Zhang, W. Conant, R. D. Cess, J. T. Kiehl, H. Grassl, and L. Shi, 1995: Warm pool budget and shortwave cloud forcing: A missing physics? Science, 267, 499-503.

Rasch, P. J., W. D. Collins, and B. E. Eaton, 2000: Understanding the Indian Ocean Experiment INDOEX aerosol distributions with an aerosol assimilation. Submitted to J. Geophys. Res.

Rose, F. G., and T. P. Charlock, 1999: Profiles of longwave fluxes in clear skies using CERES data, ECWF data, and the Fu-Liou radiative transfer code. Proceedings of the AMS Tenth Conference on Atmospheric Radiation, Madison WI (June 28 – July 2, 1999), 106-109.

Rose, F., T. Charlock, D, Rutan, and G. L. Smith, 1997: Tests of a constrainment algorithm for the surface and atmospheric radiation budget. Proceedings of the Ninth Conference on Atmospheric Radiation, Long Beach (Feb. 2-7, 1997), AMS, 466-469.

Rossow, W. B., L. C. Garder, P.-J. Lu, and A. Walker, 1991: International Satellite Cloud Climatology Project (ISCCP) documentation of cloud data. WMO/TD-No. 266, Revised March 1991, World Meteorological Organization, Geneva, 76 pp. plus three appendices.

Rutan, D., and T. Charlock, 1997: Spectral reflectance, directional reflectance, and broadband albedo of the earth's surface. Proceedings of the Ninth Conference on Atmospheric Radiation, Long Beach (Feb. 2-7, 1997), AMS, 466-469.

Rutan, D., and T. Charlock, 1999: Land surface albedo with CERES broadband observations. Proceedings of the Tenth Conference on Atmospheric Radiation, Madison WI (28 June – 2 July), 1999, AMS, 208-211.

Satheesh, S. K., V. Ramanathan, X. Li-Jones, J. M. Lobert, I. A. Podgorny, J. M. Prospero, B. N. Holben, and N. G. Loeb, 1999: A model for the natural and anthropogenic aerosols over the tropical Indian Ocean derived from Indian Ocean Experiment data. J. Geophys. Res., 104, 27,421-27,440.

Schmid, B., J. Michalsky, R. Halthore, M. Beauharnois, L. Harrison, J. Livingston, P. Russell, B. Holben, T. Eck, and A. Smirnov, 1999: Comparison of aerosol optical depth from four solar radiometers during the fall 1997 ARM Intensive Observing Period. Geophys. Res. Lett., 26, 2725-2728.

Shaw, J. A., and J. H. Churnside, 1997: Scanning-laser glint measurements of sea-surface slope statistics. Appl. Opt., 36, 4202-4213.

Soden, B. J., S. A. Ackerman, D. O'C. Starr, S. H. Melfi, and R. A. Ferrare, 1994: Comparison of upper tropospheric water vapor from GOES, Raman lidar, and CLASS sonde measurements. J. Geophys. Res., 99, 21 005-21 016.

Spinhirne, J. D., 1993: Micro Pulse Lidar. IEEE Trans. Geosc. Rem. Sens., 31, 48-55.

Suttles, J. T., R. N. Green, P. Minnis, G. L. Smith, W. F. Staylor, B. A. Wielicki, I. J. Walker, D. F. Young, V. R. Taylor, and L. L. Stowe, 1988: Angular radiation models for the earth-atmosphere system. Vol. I: Shortwave Radiation. NASA Ref. Publ. RP-1184, 147 pp.

Suttles, J. T., R. N. Green, G. L. Smith, W. F. Staylor, B. A. Wielicki, I. J. Walker, V. R. Taylor, and L. L. Stowe, 1989: Angular radiation models for the earth-atmosphere system. Vol. I: Longwave Radiation. NASA Ref. Publ. RP-1184, Vol. II, 87 pp.

Stamnes, K., S.-C. Tsay, W. Wiscombe, and K. Jayaweera, 1988: Numerically stable algorithm for discrete-ordinates-method radiative transfer in multiple scattering and emitting layered media. Appl. Opt., 27, 2502-2509.

Stephens, G. L., and S.-C. Tsay, 1990: On the cloud absorption anomaly. Q. J. R. Meteorol. Soc., 116, 671-704.

Stokes, G. M., and S. E. Schwartz, 1994: The Atmospheric Radiation Measurement Program (ARM) Program: Programmatic Background and Design of the Cloud and Radiation Test Bed. Bull. Amer. Meteor. Soc., 75, 1201-1221.

Stowe, L. L., A. M. Ignatov, and R. R. Singh, 1997: Development, validation, and potential enhancements to the second generation operational aerosol product at the National Environmental Satellite, Data, and Information Service of the National and Oceanic Atmospheric Administration. J. Geophys. Res., 102, 16,923-16,934.

Stuhlmann, R., E. Raschke, and U. Schmid, 1993: Cloud generated radiative heating from METEOSAT data. IRS '92: Current Problems in Atmospheric Radiation. (Proceedings of International Radiation Symposium, Tallinn, Estonia, 3-8 August 1992) A. Deepak Publishing, Hampton, Virginia, 69-75.

Tegen, I., and A. A. Lacis, 1996: Modeling of particle size distribution and its influence on the radiative properties of mineral dust aerosol. J. Geophys. Res., 101, 19,237-19,244.

Valero, F. P. J., R. D. Cess, M. Zhang, S. K. Pope, A. Bucholtz, B. Bush, and J. Vitko, 1997: Absorption of solar radiation by the cloudy atmosphere: Interpretations of collocated aircraft measurements. J. Geophys. Res., 102, 29,917-29,927.

Valero, F. P. J., P. Minnis, S. K. Pope, A. Bucholtz, B. C. Bush, D. R. Doelling, W. L. Smith, Jr., and X. Dong, 2000: The absorption of solar radiation by the atmosphere as determined using satellite, aircraft, and surface data during the ARM Enhanced Short-wave Experiment (ARESE). J. Geophys. Res., 105, 4743-4758.

Wentz, Frank J., C. Gentemann, D. Smith, and D. Chelton, 2000: Satellite measurements of sea-surface temperature through clouds. Science, 288, 847-850.

Whitlock, C. H., T. P. Charlock, W. F. Staylor, R. T. Pinker, I. Laszlo, A. Ohmura, H. Gilgen, T. Konzelman, R. C. DiPasquale, C. D. Moats, S. R. LeCroy, and N. A. Ritchey, 1995: First global WCRP shortwave Surface Radiation Budget dataset. Bull. Amer. Meteor. Soc., 76, 905-922.

Whitlock, C. H., S. R. LeCroy, and R. J. Wheeler, 1994: Narrowband angular reflectance properties of the alkali flats at White Sands, New Mexico. Remote Sens. Environ., 50, 171-181.

Wielicki, B. A., and B. Barkstrom, 1991: Clouds and the Earth's Radiant Energy System (CERES): An Earth Observing System Experiment. Second Symposium on Global Change Studies, New Orleans, LA, Jan. 14-18, 1991, pp. 11-16.

Wielicki, B. A., R. D. Cess, M. D. King, D. A. Randall, and E. F. Harrison, 1995: Mission to Planet Earth: Role of clouds and radiation in climate. Bull. Amer. Meteor. Soc., 76, 2125-2153.

Wielicki, B. A., and R. N. Green, 1989: Cloud identification for ERBE radiative flux retrieval. J. Appl. Meteor., 28, 1133-1146.

Wild, M., A. Ohmura, H. Gilgen, and E. Roeckner, 1995: Validation of general circulation model radiaive fluxes using surface observations. J. Climate, 8, 1309-1324.

Wild, M., A. Ohmura, H. Gilgen, E. Roeckner, M. Giorgetta, and J.-J. Morcrette, 1998: The disposition of radiative energy in the global climate system: GCM-calculated versus observational estimates. Climate Dynamics, 14, 853-869.

Wild, M., 1999: Discrepancies between model-calculated and observed shortwave atmospheric absorption in areas with high aerosol loadings. J. Geophys. Res., 104, 27,361-27,373.

Whitlock, C. H., T. P. Charlock, W. F. Staylor, R. T. Pinker, I. Laszlo, A. Ohmura, H. Gilgen, T. Konzelman, R. C. DiPasquale, C. D. Moats, S. R. LeCroy, and N. A. Ritchey, 1995: First global WCRP shortwave Surface Radiation Budget dataset. Bull. Amer. Meteor. Soc., 76, 905-922.

Whitlock, C. H., S. R. LeCroy, and R. J. Wheeler, 1994: Narrowband angular reflectance properties of the alkali flats at White Sands, New Mexico. Remote Sens. Environ., 50, 171-181.

Yang, S.-K., S. Zhou, and A. J. Miller, 2000: SMOBA: A 3-dimensional daily ozone analysis using SBUV/2 and TOVS measurements.
www.cpc.ncep.gov/products/stratosphere/SMOBA/smoba_doc.html

Yarosh, E. S., C. F. Ropelewski, and K. E. Mitchell, 1996: Comparisons of humidity observations and Eta model analyses and forecasts for water balance studies during GIST. J. Geophys. Res., 101, 23,289-23,298.

Zender, C. S., B. Bush, S. K. Pope, A. Bucholtz, W. D. Collins, J. T. Kiehl, F. P. Valero, and J. Vitko, Jr., 1997: Atmospheric absorption during the Atmospheric Radiation Measurement (ARM) Enhanced Shortwave Experiment (ARESE). J. Geophys. Res., 102, 29,901-29916.